

THE SOLAR WIND

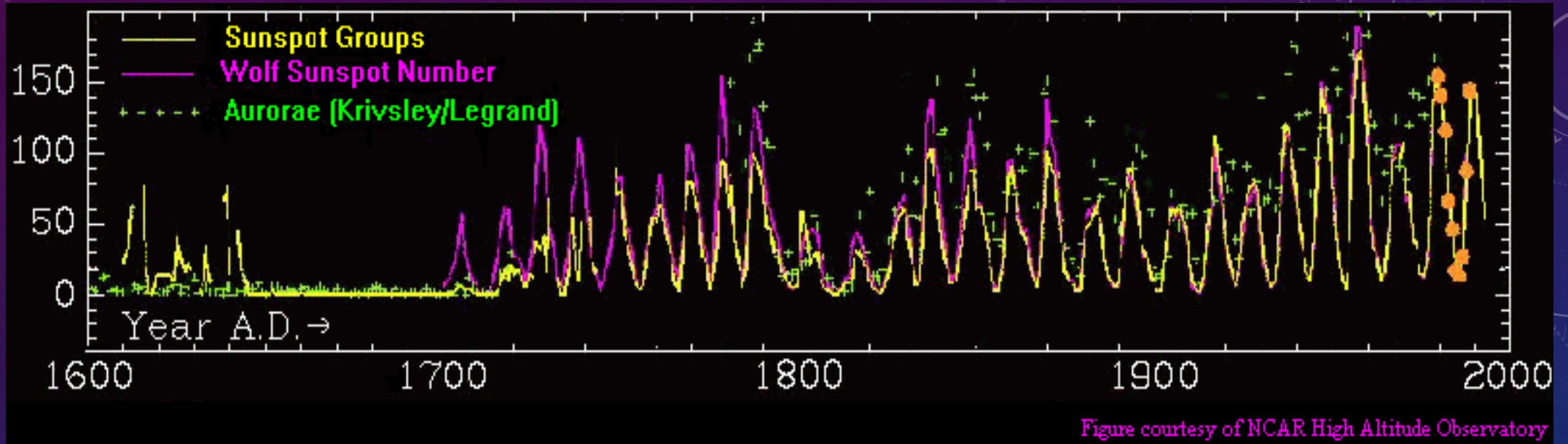
M2 PPF – E3 – 2025

ARNAUD ZASLAVSKY

arnaud.zaslavsky@sorbonne-universite.fr

arnaud.zaslavsky@obspm.fr

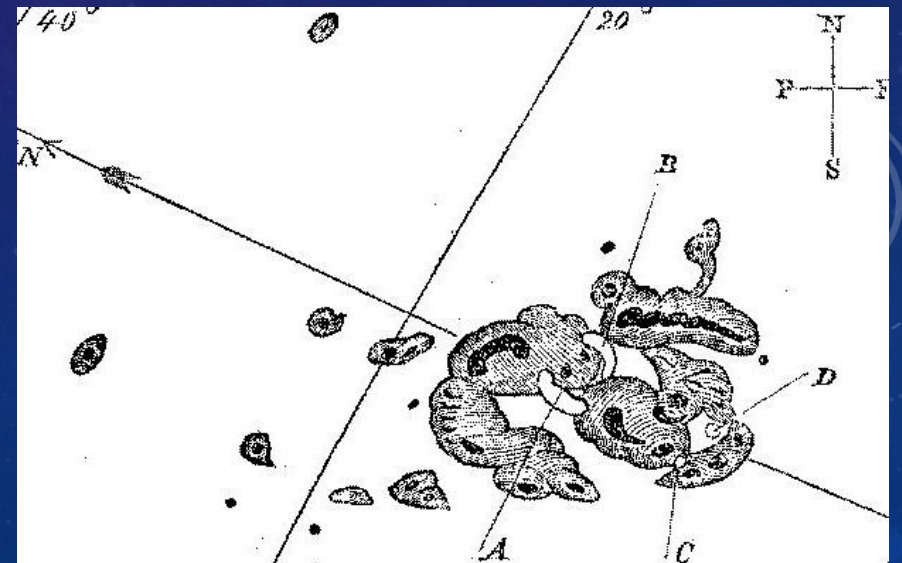
A BRIEF HISTORY: THE FIRST IDEAS



1859: Richard Carrington drew spots from a projected image of the Sun and observed a sharp increase in luminosity: an eruption.

Strong auroral phenomena are observed 17 hours later. Carrington proposes a link between these events.

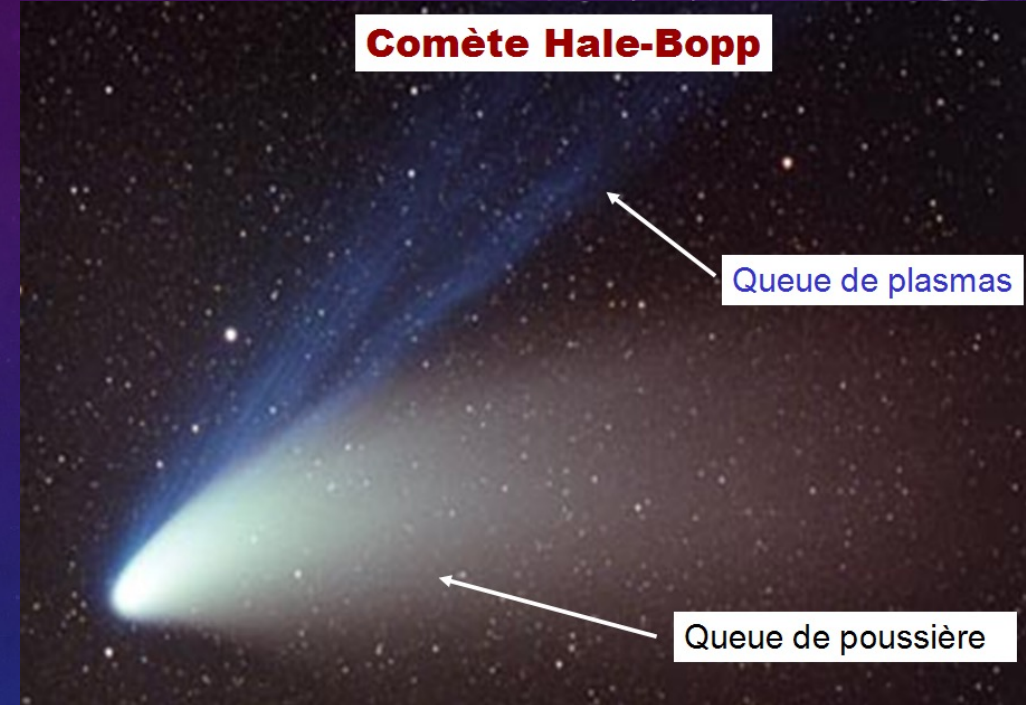
1900: Kristian Birkeland proposes that 'The Earth is permanently bombarded by electric corpuscles emitted by the Sun. emitted by the Sun' (discovery of e^- in 1897)



A BRIEF HISTORY: THE 50'S

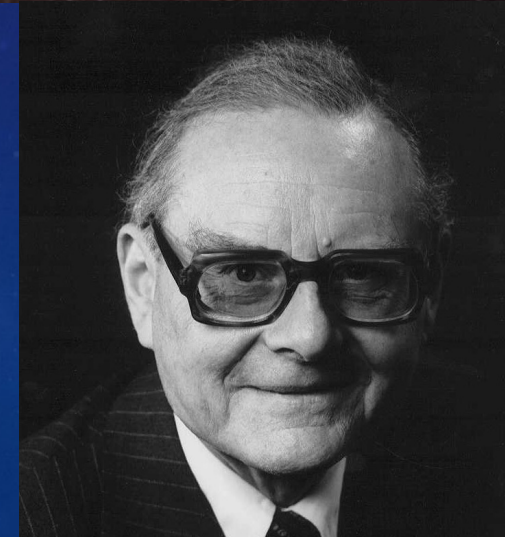
Sydney Chapman

- Because the corona is very hot and very conductive, the heat should be present at a great distance
=> A very large static atmosphere
- The Earth orbits in the Sun's static corona

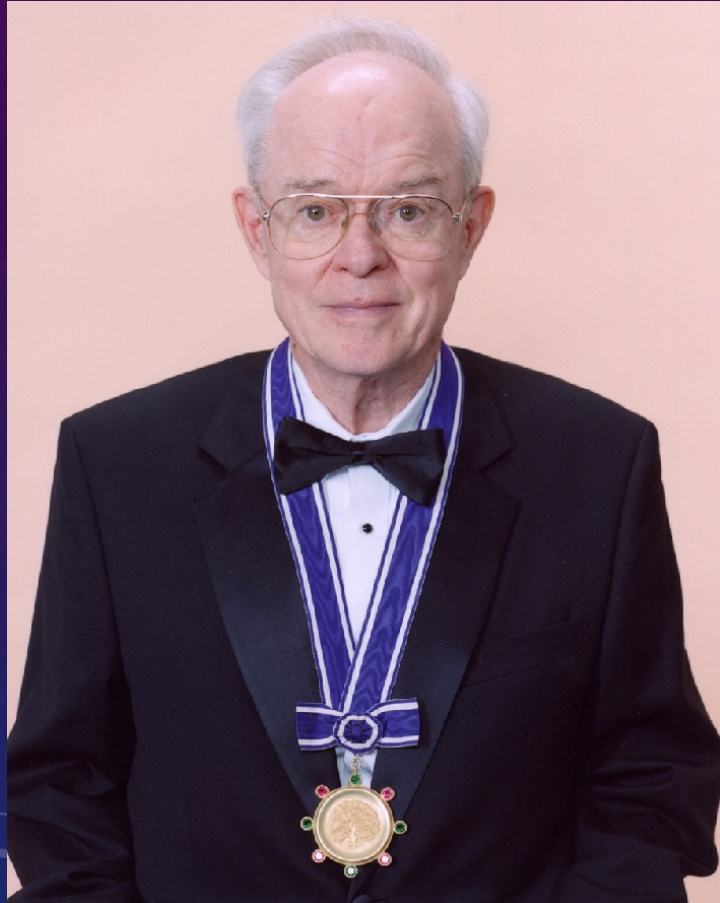


Ludwig Biermann: observation of comets.

Suggested that the plasma tail was due to the solar wind, and measured 'blobs' flowing at speeds of around 100 km/s.



UN BREF HISTORIQUE : LES DEBUTS DU SPATIAL



In 2003, Eugene Parker was awarded the Kyoto Prize for Basic Science for predicting the existence of a supersonic solar wind in 1958.

First Soviet probe (Luna 2) lands on the Moon in 1959.

Measurement of supersonic ion flux.

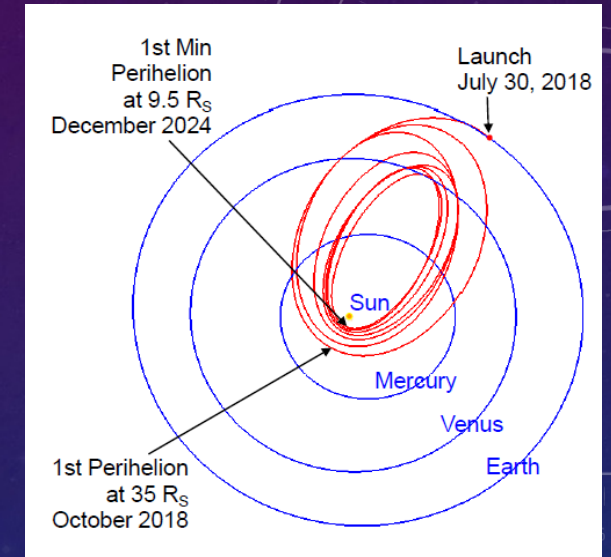
Mariner 2 (1962) on its way to Venus made the first directional measurements of the solar wind.

1959 : Luna 2 (flux d' ions, pas de direction)

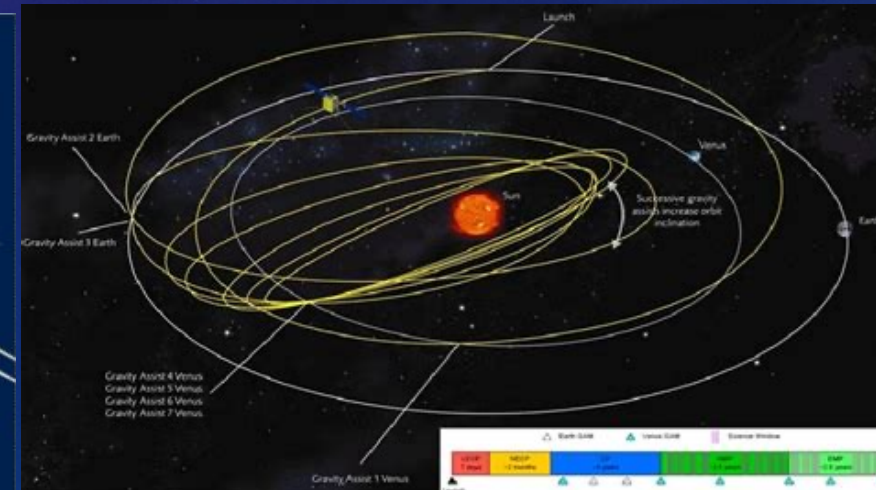


AUJOURD'HUI...

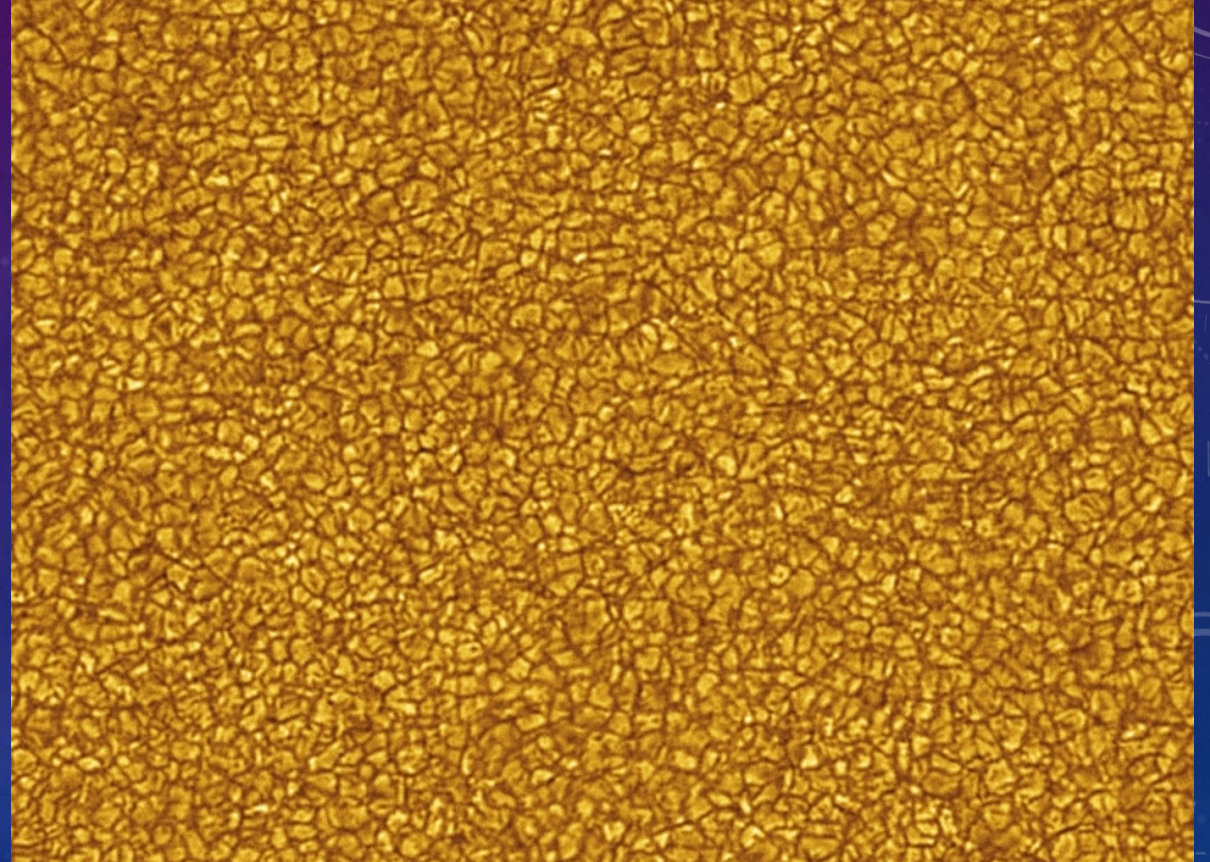
- Numerous probes have been launched, and a great deal of data has been collected.
- In-situ observations of the interplanetary plasma + Observation of the solar corona in many wavelengths



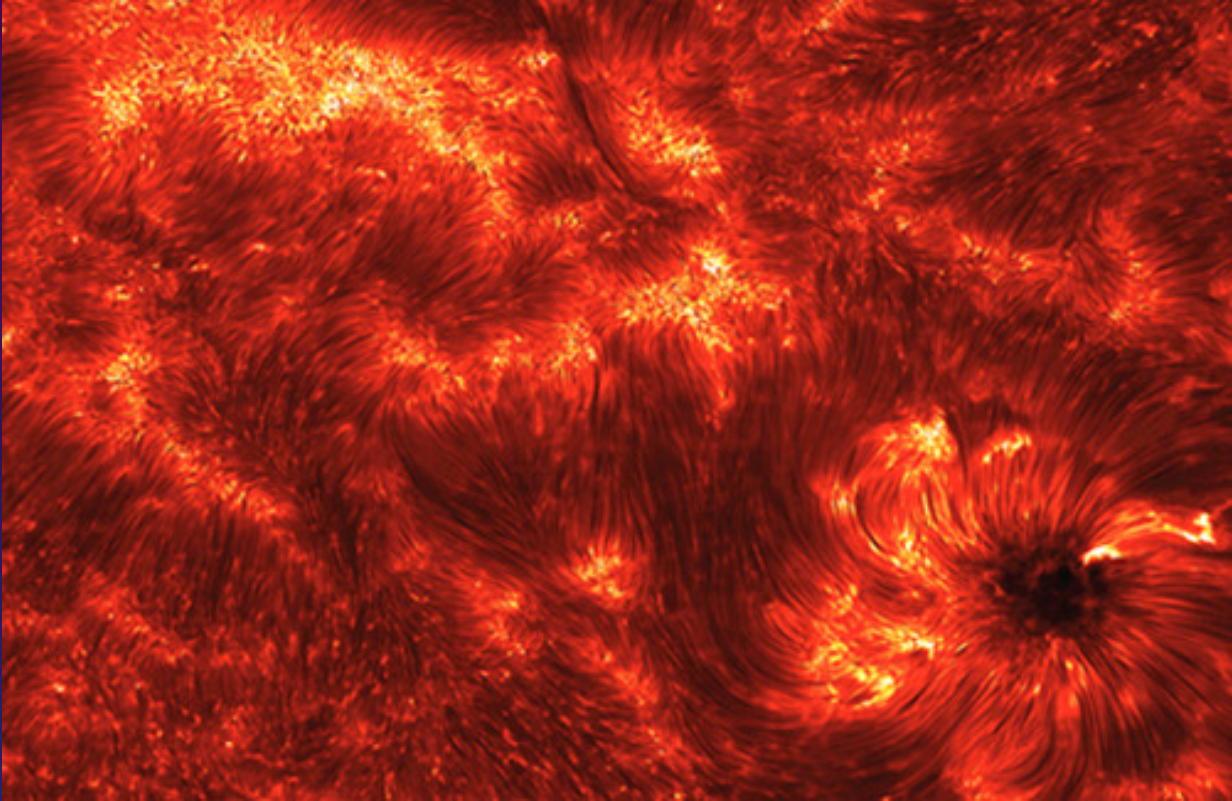
- Parker Solar Probe (NASA, launched Aug. 2018)
- Solar Orbiter probe (ESA, launched Nov. 2019)



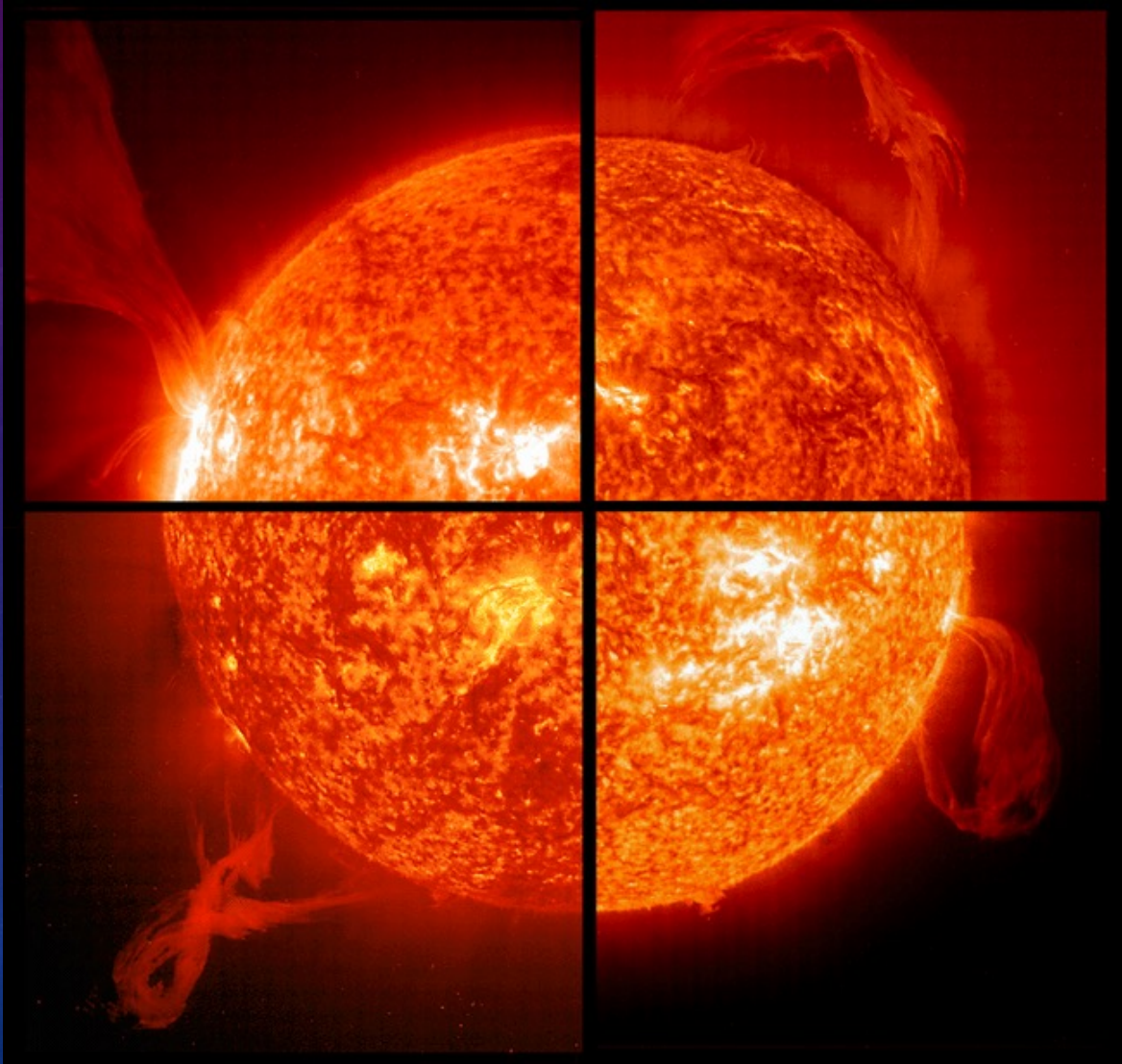
PHOTOSPHERE



CHROMOSPHERE



SDO, He II, 30.4 nm

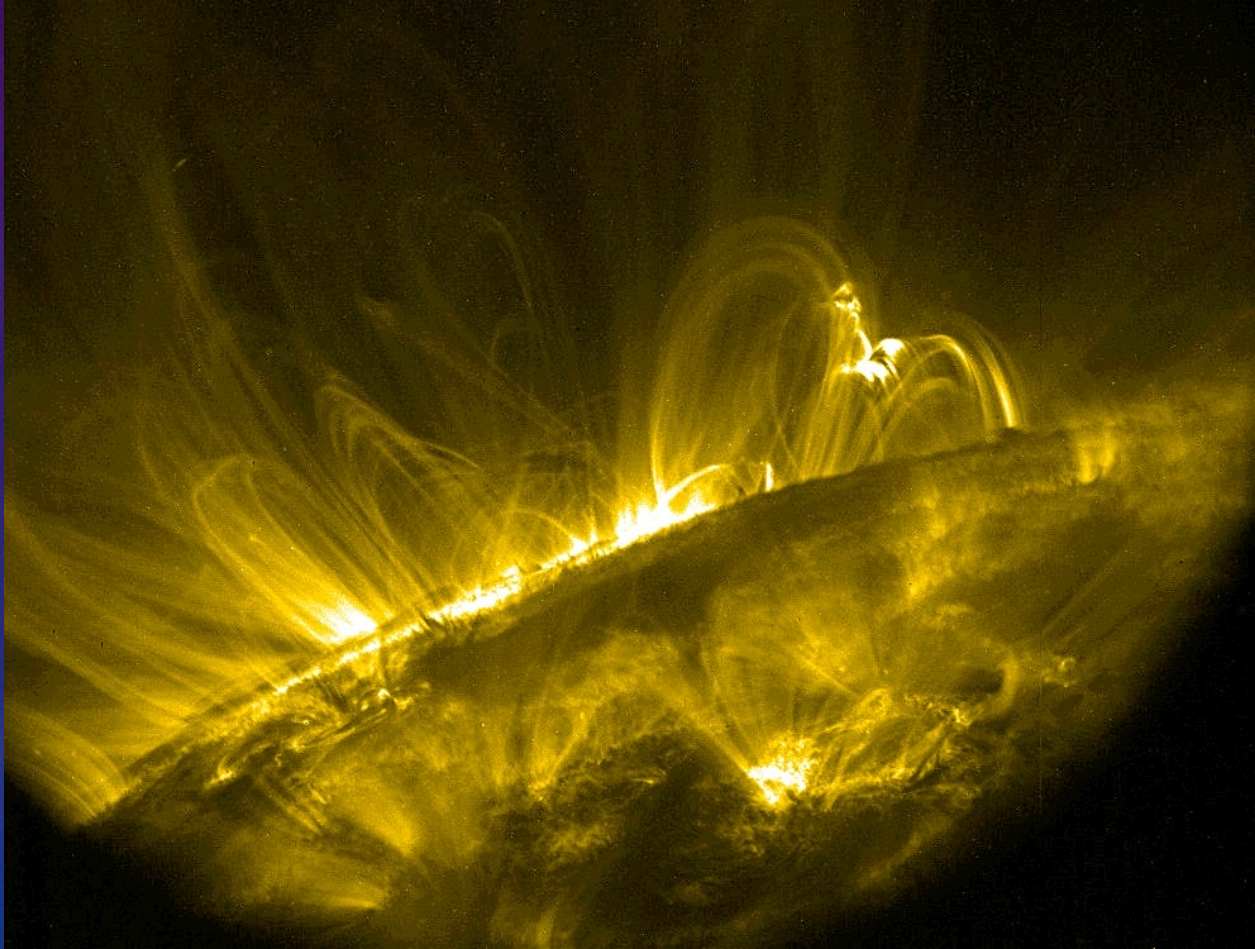


SOHO/EIT

CORONA

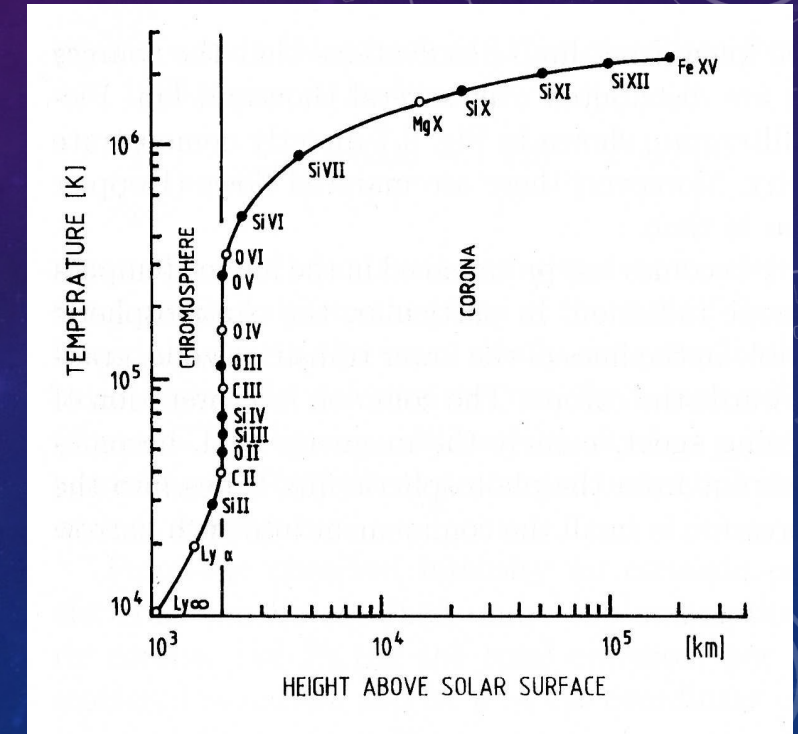
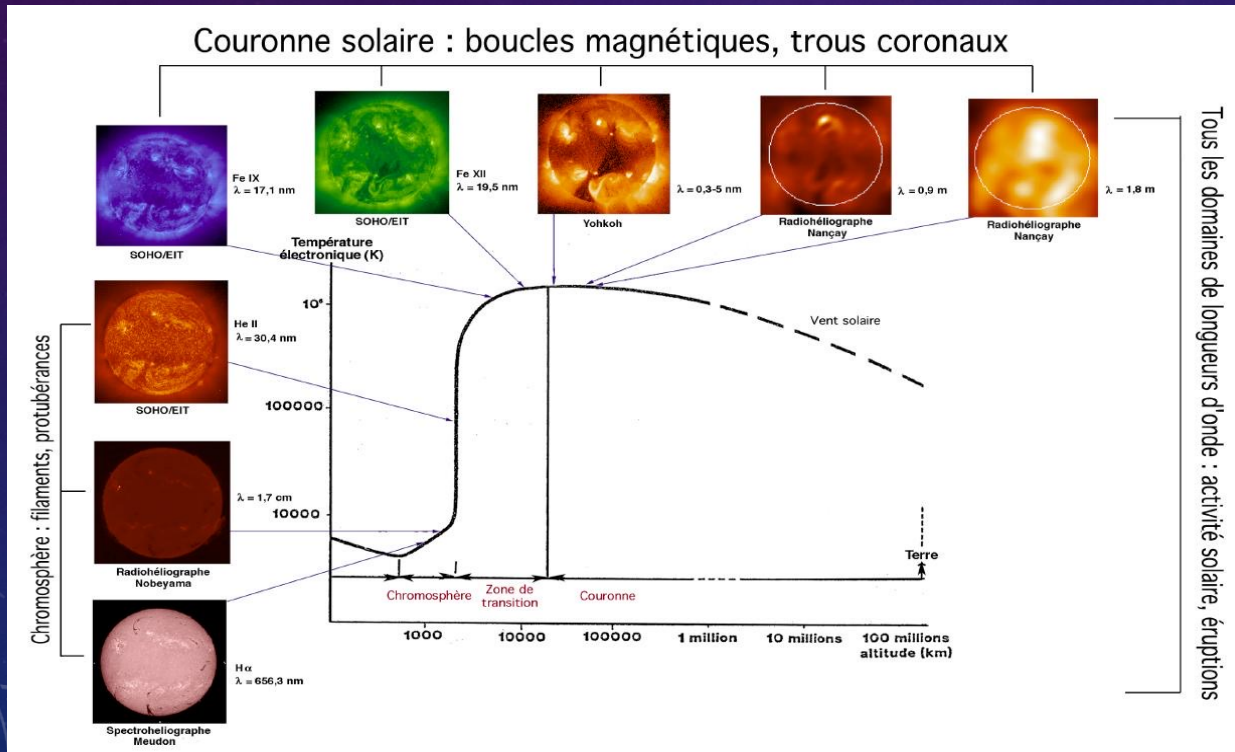


© 2017 Miloslav Druckmüller, Peter Aniol, Shadia Habbal



QUIET SOLAR ATMOSPHERE: THE TRANSITION REGION

- Thin layer: thickness still poorly known but $< 100\text{km}$
- Extreme temperature gradient: rise from 2×10^4 to 10^6 K
- Density: 10^9 to 10^{10} atoms/cm³ (5×10^{-15} to 5×10^{-14} g/cm³)
- Abrupt transition between chromospheric and coronal physical conditions
- Abrupt transition in the appearance of the Sun (emissive regions)



Temperature profile and emission lines typical of RT.

THERMAL INSTABILITY IN THE TRANSITION REGION

Steady-state heat balance:

$$\text{div } j_c = Q_c - Q_{\text{ray}}$$

j_c : Heat flux density

Q_c : Heating term

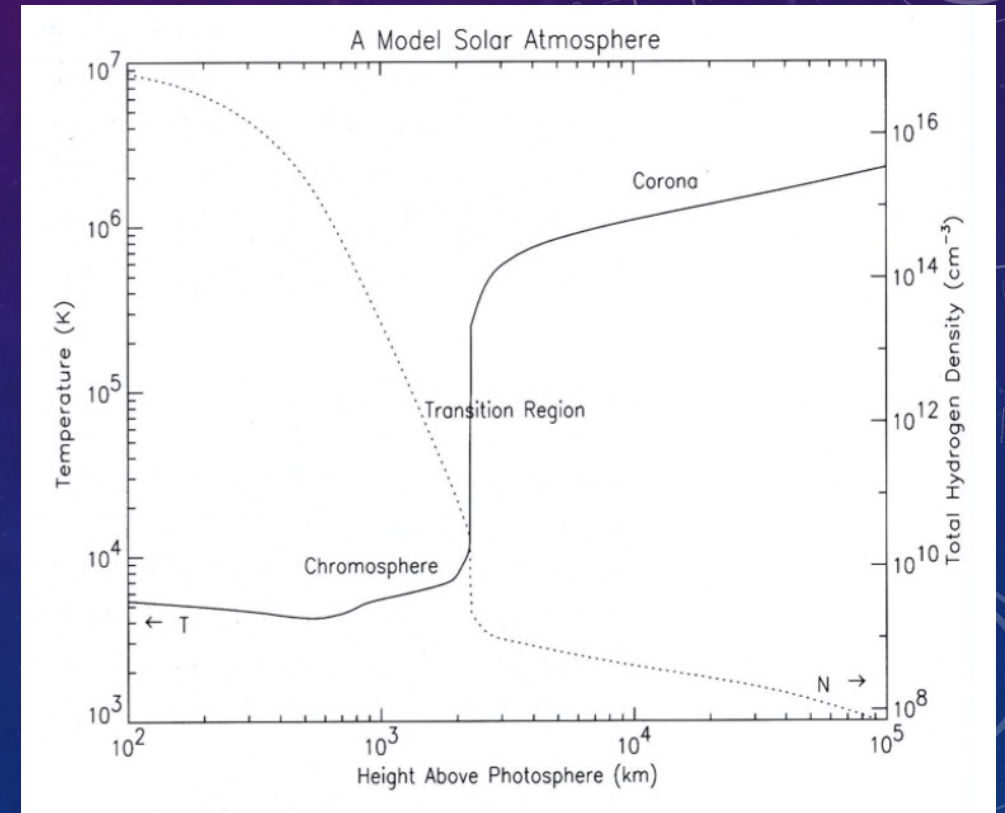
Q_{ray} : Radiative cooling term

j_c is linked to the temperature gradient by a Fourier type law

$$j_c = -\kappa \nabla T$$

Where the thermal conductivity (to be discussed) is given by

$$\kappa = K_0 T^{5/2}, \quad \text{avec } K_0 \simeq 5,6 \times 10^{-12} \text{ W.m}^{-1}\text{K}^{-7/2}$$



Div j_c is weak in chromospheric conditions (cold)

Div j_c is strong in coronal conditions

HEAT BALANCE IN THE CHROMOSPHERE

Neglecting the conduction term, we see that the temperature is determined by the local balance between heating and radiative cooling.

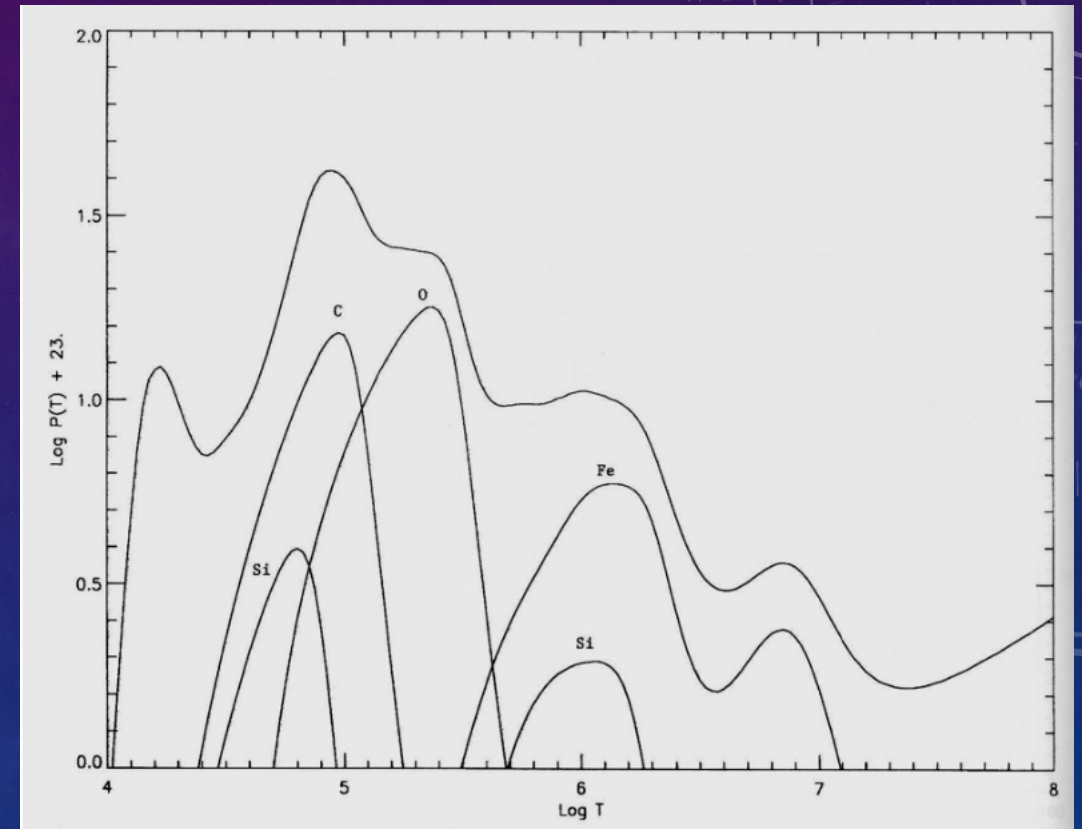
$$\Lambda(T) \simeq \frac{Q_c}{n_e^2}$$

Density decreases with height (stratification by solar gravity): the RH term increases (more or less) exponentially.

On the other hand, the efficiency of radiative cooling decreases from a temperature of about 10^5 K.

Below a critical density, radiative losses can no longer compensate for heating.

$$n_e \simeq \left(\frac{Q_c}{\Lambda_{max}} \right)^{1/2} \sim \left(\frac{Q_c}{1 \text{ W.m}^{-3}} \right)^{1/2} 10^{17} \text{ m}^{-3}$$



STABILISATION BY CONDUCTION IN THE CORONA

The temperature rises sharply from the height at which the critical density is reached.

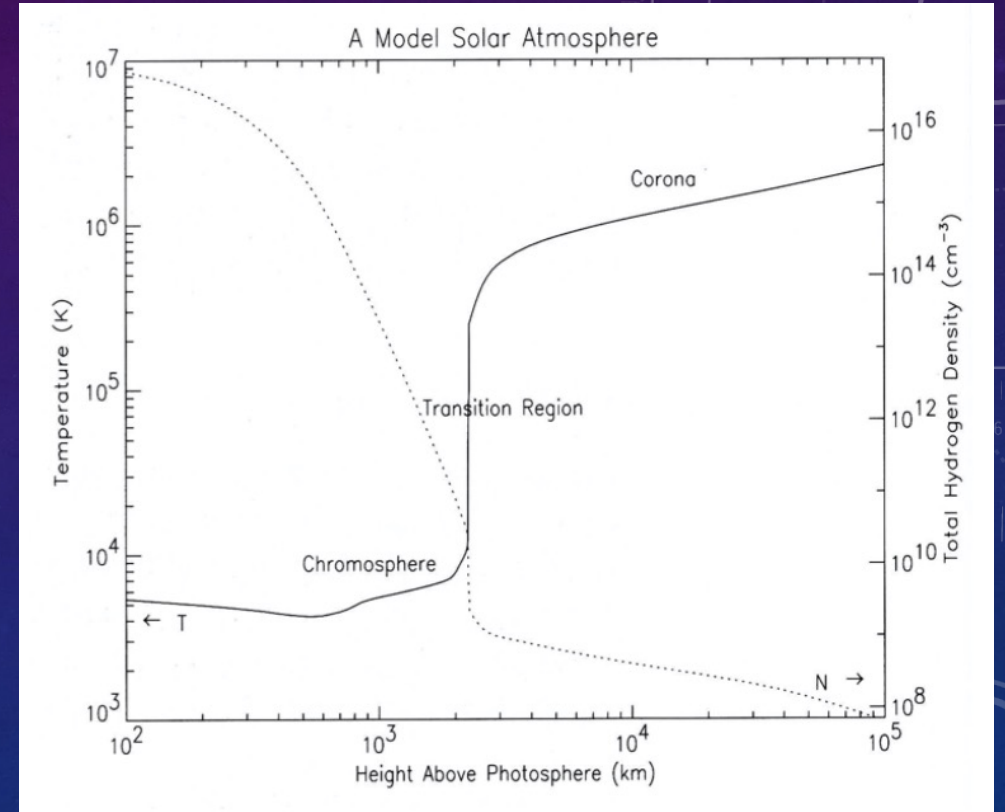
This instability stabilises at a temperature where conduction becomes important (conductivity is a sensitive function of T).

Approximation: radiative cooling at the top of the RT is totally neglected.

The value of the coronal temperature is :

$$T_{\text{couronne}} \simeq \left(\frac{L^2}{K_0} Q \right)^{2/7} \sim \left(\frac{Q_c}{1 \text{ W.m}^{-3}} \right)^{2/7} 10^6 \text{ K}$$

That's about the million-degree temperature observed if Q_c is of the order of Watt per cubic metre.



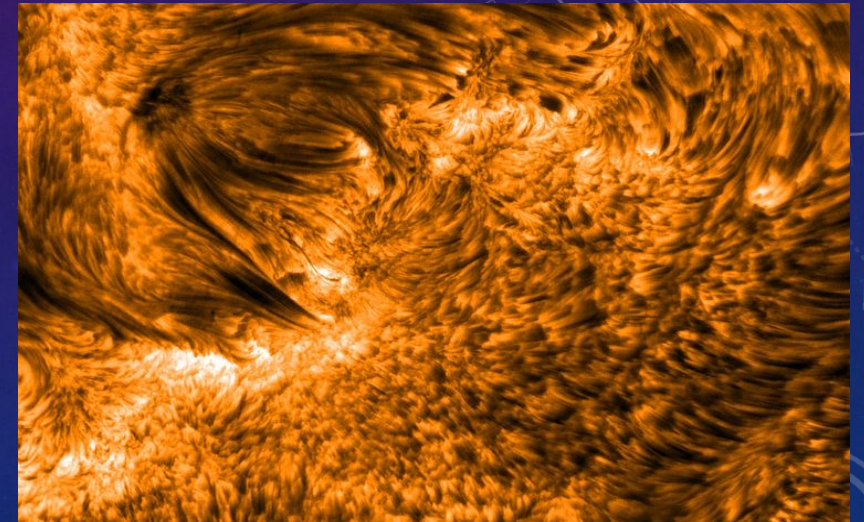
(Very) rudimentary model for $Q = 1\text{W/m}^3$:
 $n_{\text{crit}} = 10^{11} \text{ cm}^{-3}$
 $T = 10^6 \text{ K}$

CORONAL HEATING: IDENTIFYING THE ENERGY SOURCE

- First hypothesis: hydrodynamic heating
- Dissipation of acoustic waves produced by photospheric turbulent convection in a non-magnetic medium (chromospheric lattice cells):
- Wave energy density:

$$E = \frac{1}{2} \rho \delta u^2$$

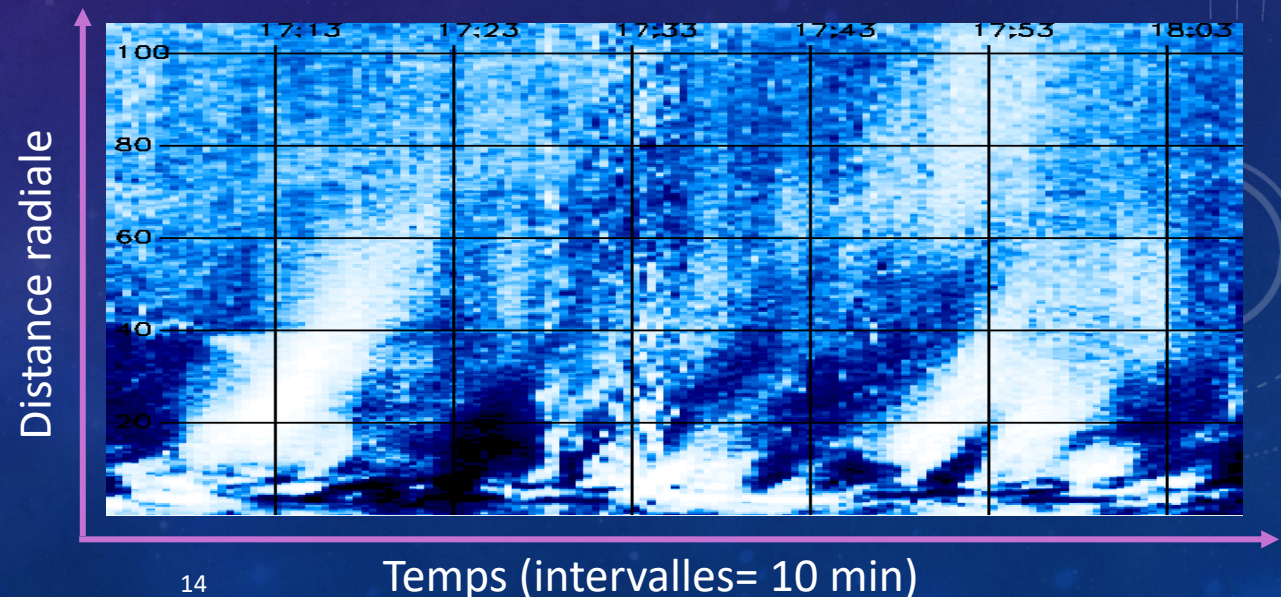
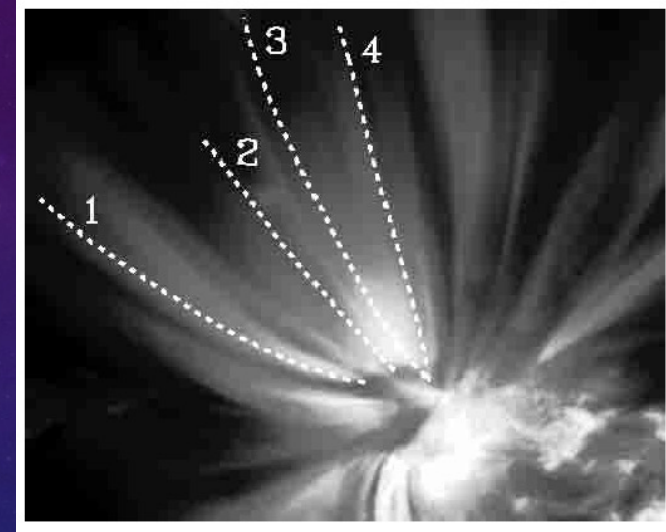
- Due to the negative density gradient, the waves are transformed into shock waves and dissipated in the form of heat.
- Very efficient process in the chromosphere
- Energy does not reach the corona
- Acoustic heating may be important for other stars



CORONAL HEATING: IDENTIFYING THE ENERGY SOURCE

Magneto-acoustic waves

- Progressive perturbations (Ampl.: 5 to 10%) detected in large-scale loops emerging at the edge of an active region (SOHO/EIT, TRACE):
- Quasi-period: 5 min
- Propagation speed: 60 to 180 km/s \sim cs
- Slow magneto-acoustic waves
 - The different speeds observed in the same loops in different lines suggest the presence of unresolved fine loops at different temperatures.

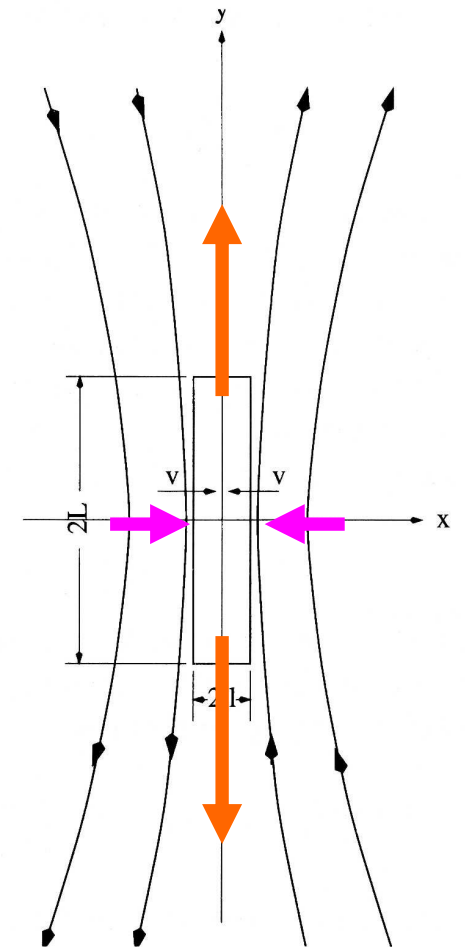


Robbrecht et al. 1999, 2001

CORONAL HEATING: IDENTIFYING THE ENERGY SOURCE

- At points where opposing field lines converge, small-scale current sheets form:
 - Example of 'X point' topology
 - High Ohmic dissipation in the sheet and reconnection of the magnetic field lines
- Same cause as MHD waves: random displacement of the feet of the magnetic lines
- Important distinction:
 - Waves: The magnetic field is a passive container (Propagation along the field lines)
 - Reconnection: The magnetic field plays a direct role in dissipation

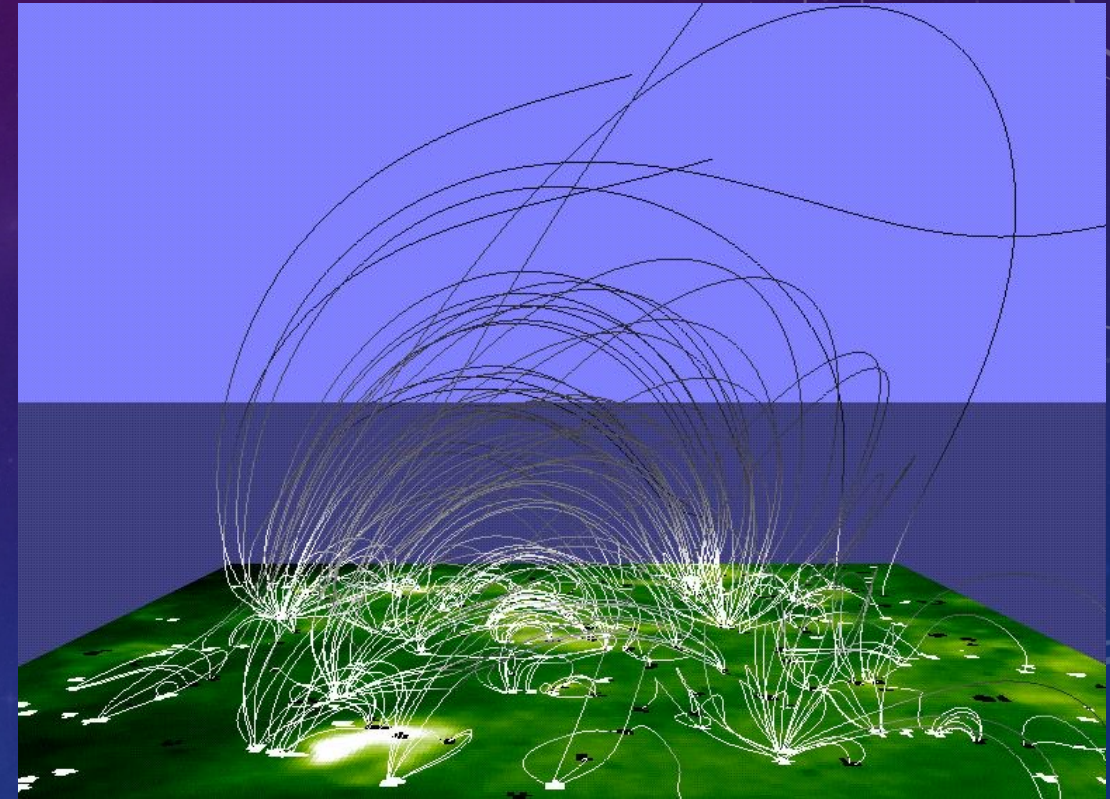
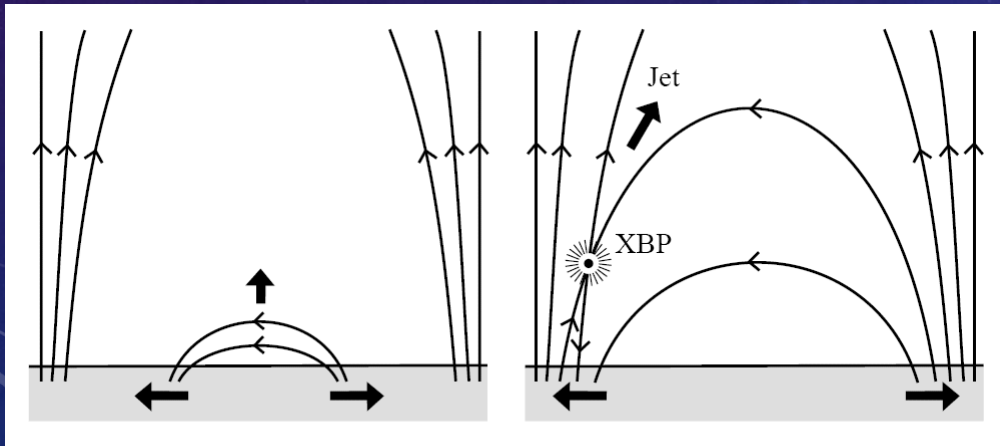
Figure 9.4 Magnetic reconnection at a neutral sheet; \mathbf{B} reverses direction along the y -axis leading to a current j_z in the z -direction. Inflow of magnetic field at velocity v is balanced by fluid outflow along the x -direction. Diagram on right shows magnetic field configuration in the Petschek geometry, including standing waves.



Références: Sturrock 1986, Bray et al. 1991, Priest

CORONAL HEATING: IDENTIFYING THE ENERGY SOURCE

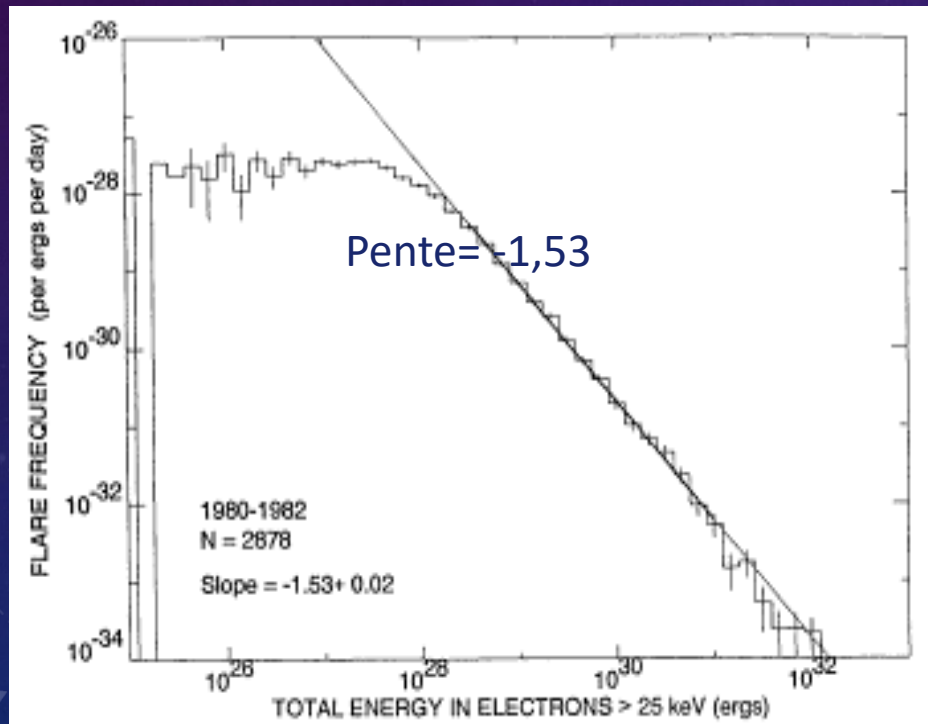
- A continuous source of heating must be present over the entire surface of the Sun
- Active regions provide only an insufficient source, localised in space and time.
- Importance of small-scale reconnections within a network of low loops covering the whole of the quiet Sun: the magnetic carpet (Title & Schrijver 1998).



Magnetic carpet covering the entire surface of the Sun.

CORONAL HEATING: IDENTIFYING THE ENERGY SOURCE

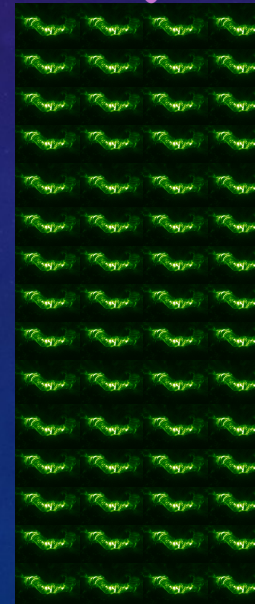
- Flares on very small space-time scales (motivation to increase resolution)
- Micro- and nano-eruptions are the continuous low-energy extension (weak, localised magnetic fields) of the spectrum of solar flares occurring in active regions (strong, large-scale magnetic fields).



Crosby et al. 1993

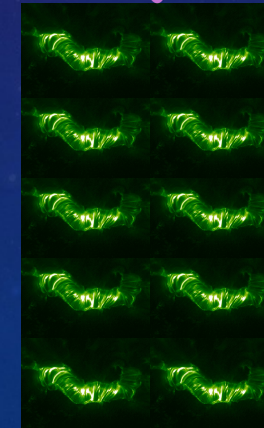
Statistics on
50,000 flares
from 1976 to
2000
(X flux, GOES)

3.6/jour



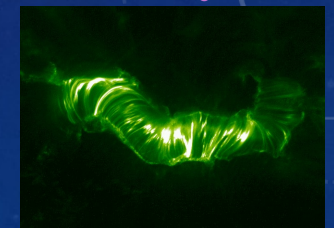
C-flares

0.5/jour



M-flares

0.04/jour



X-flares

IMPOSSIBILITY OF A STATIC SOLAR CORONA

Hydrostatic equation for the atmosphere in the gravity field in $1/r^2$:

$$p(r) = p(r_0) \exp \left(-\frac{mMG}{k} \int_{r_0}^r \frac{dr}{T(r)r^2} \right)$$

Limit on the shape of the temperature profile $T = T_0 (r/r_0)^{-a}$.

If $a < 1$, non-zero pressure at infinity.

$$T(r) \propto r^{-2/7}$$

Estimated profile with SB conductivity:

Non-zero pressure at infinity (gravity alone does not ensure containment)

$$p_\infty = p(r_0) \exp \left(-\frac{mMG}{kT_0} \frac{1}{r_0(1-\alpha)} \right) \simeq p(r_0) \exp \left(-\frac{10^7 \text{ K}}{T_0(1-\alpha)} \right)$$

Temperature and a -index required for static confinement by the interstellar medium :

$$(1-\alpha)T_{stat} \sim \frac{10^7}{\ln(p(r_0)/p_{is})} \sim 5 \times 10^5 \text{ K}$$

Not verified for the solar corona.

THE SOLAR WIND: PARKER MODEL

Conservation equations along the radial (no B field or radial B field) :

$$\frac{d}{dr} (r^2 n_e u_e) = 0, \quad \frac{d}{dr} (r^2 n_p u_p) = 0$$

$$n_e m_e u_e \frac{d}{dr} u_e = -\frac{dp_e}{dr} - e n_e E - n_e m_e \frac{GM}{r^2}$$

$$n_p m_p u_p \frac{d}{dr} u_p = -\frac{dp_p}{dr} + e n_p E - n_p m_p \frac{GM}{r^2}$$

Quasi-neutrality + no radial current : the electric field can be eliminated. We obtain :

$$n m_p u \frac{d}{dr} u = -\frac{d}{dr} (n k (T_e + T_p)) - n m_p \frac{GM}{r^2} \quad (1)$$

(Isothermal closure)

We reformulate eq.(1) with the help of the continuity equation :

$$(u^2 - c_s^2) \frac{1}{u} \frac{d}{dr} u = \frac{2c_s^2}{r} \left(1 - \frac{r_c}{r}\right)$$

THE SOLAR WIND: PARKER MODEL

$$\frac{u^2}{2} - c_s^2 \ln u = 2c_s^2 \ln r + 2c_s^2 \frac{r_c}{r} + C$$

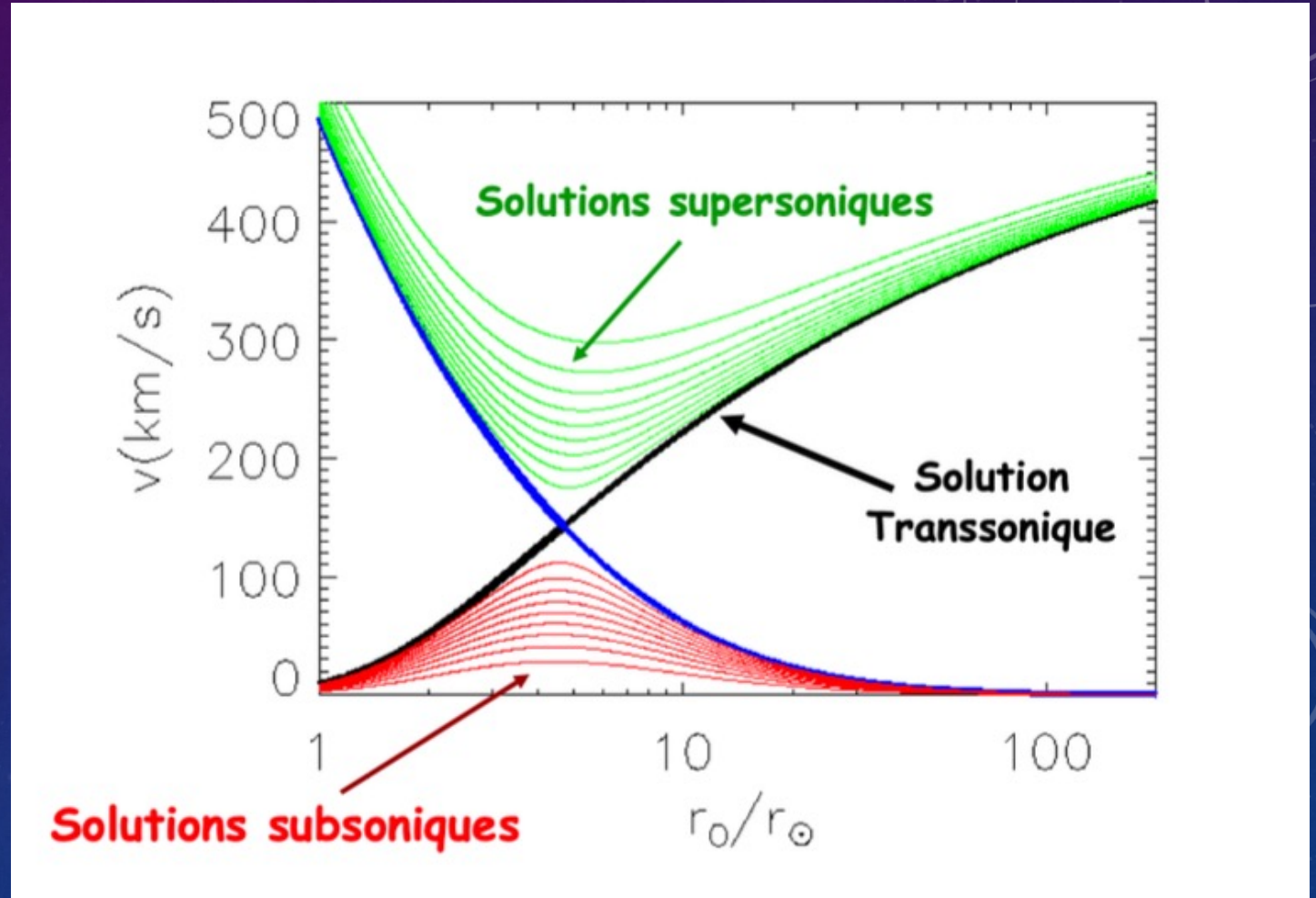
Different families of solution.

The physically realised solution is the transonic solution ($C = -3c_s^2/2$)

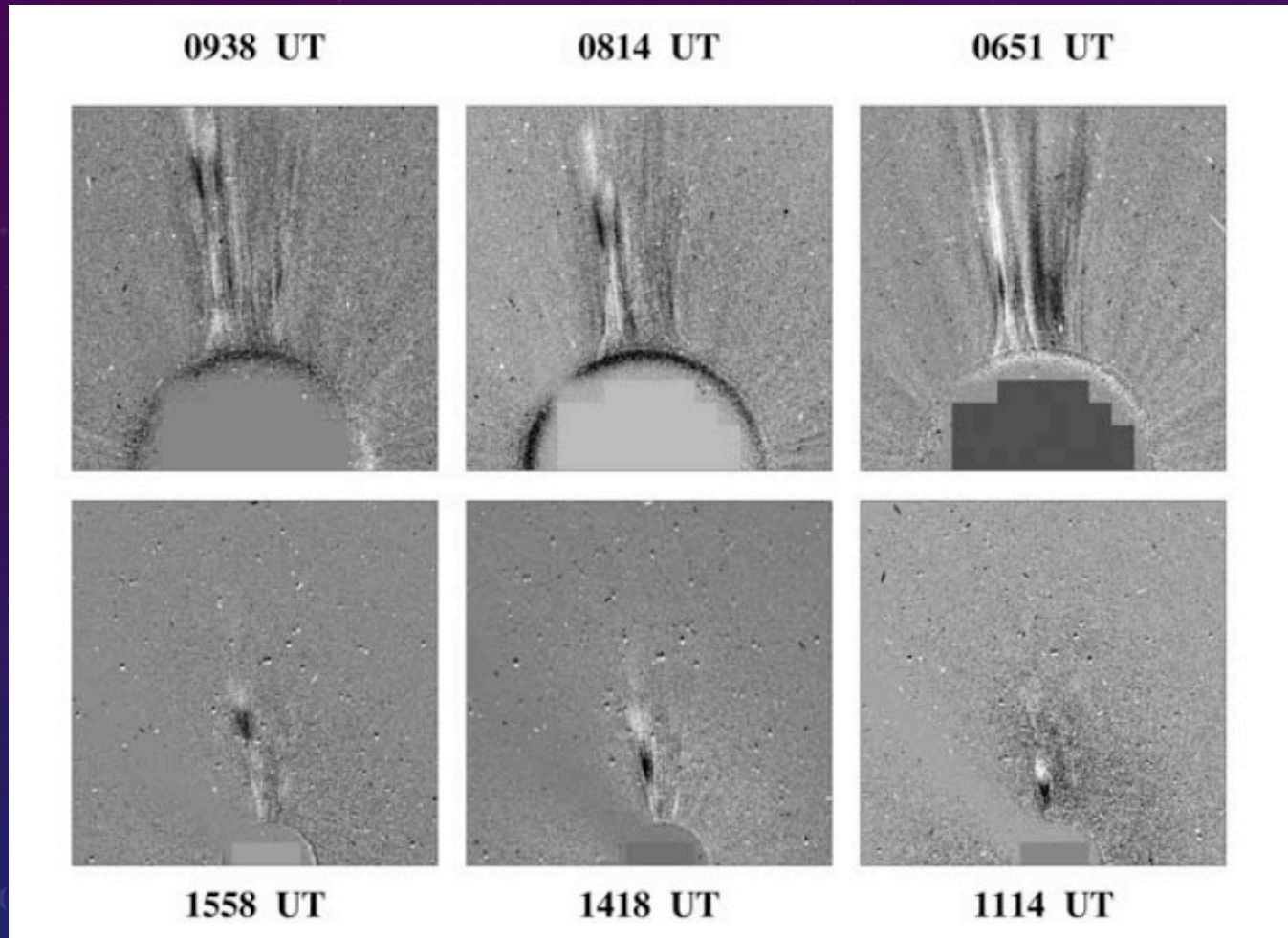
Critical radius and terminal velocity :

$$r_c \simeq \frac{GMm_p}{4kT} \simeq 2,9 \left(\frac{10^6 \text{ K}}{T} \right) R_s$$

$$u_\infty \simeq 1,5 \left(\frac{4kT}{m_p} \right)^{1/2} \simeq 272 \left(\frac{T}{10^6 \text{ K}} \right)^{1/2} \text{ km.s}^{-1}$$

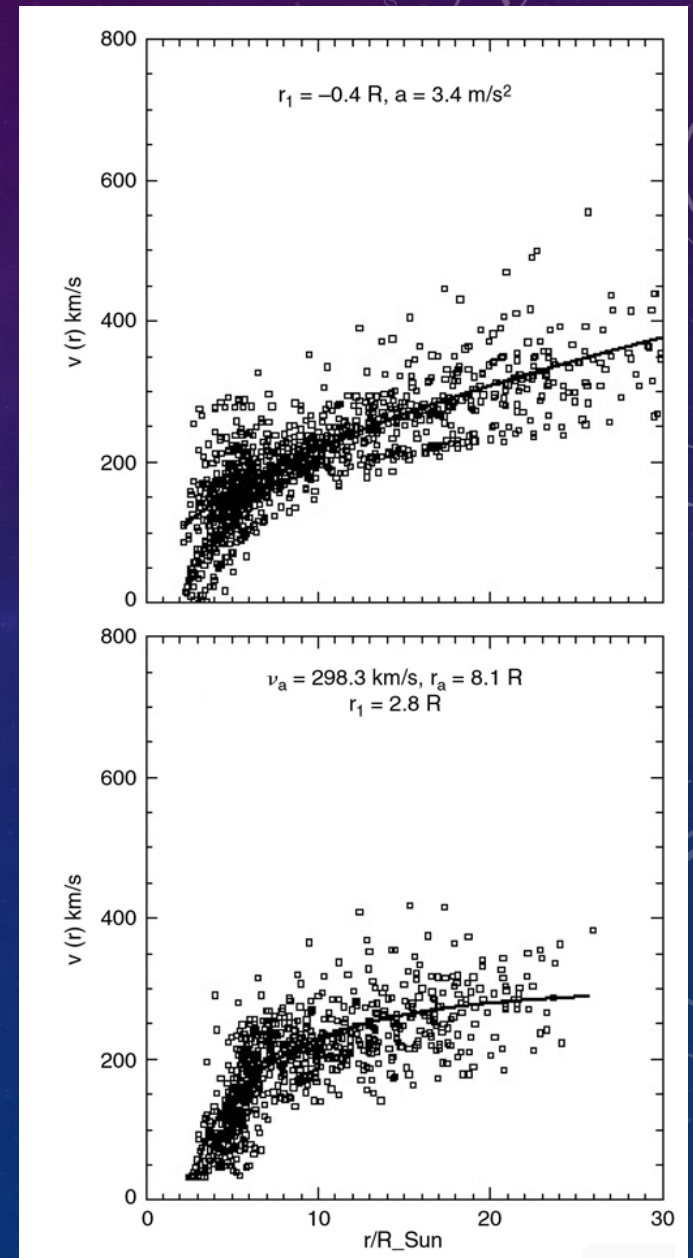


THE SOLAR WIND: ACCELERATION

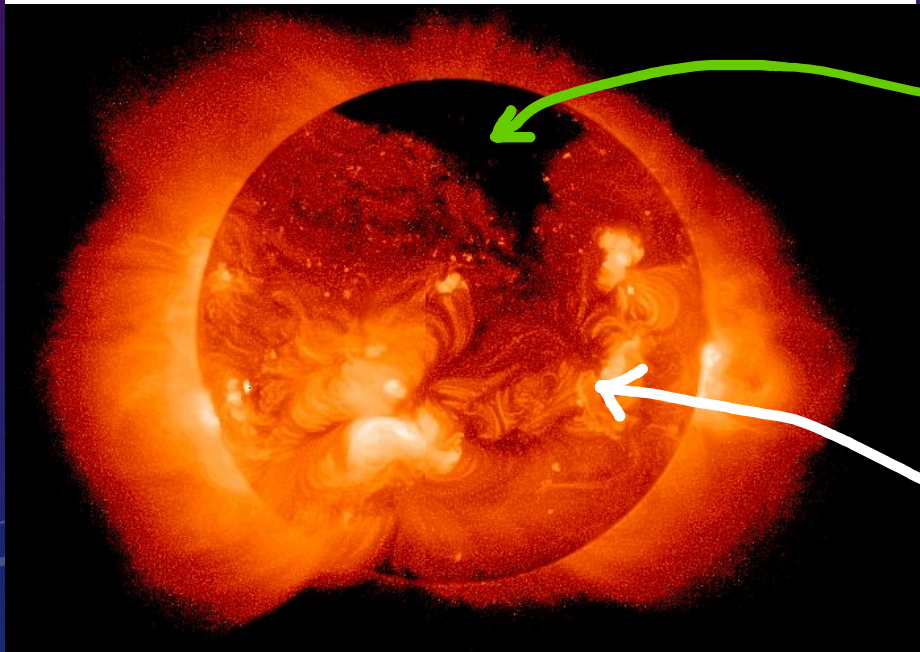
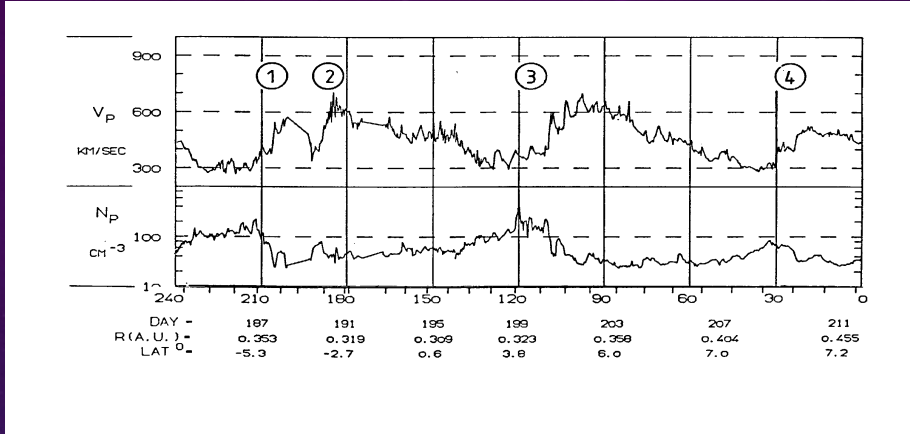


Lumière blanche

Sheeley et al., 1997



SOLAR WIND: SPACE OBSERVATIONS (HELIOS)



Yohkoh

Composition :

- e^-
- H^+ : ~95%
- He^{2+} : ~4%
- ~1% d' ions lourds (C, N, O, Ne, Mg, Fe)

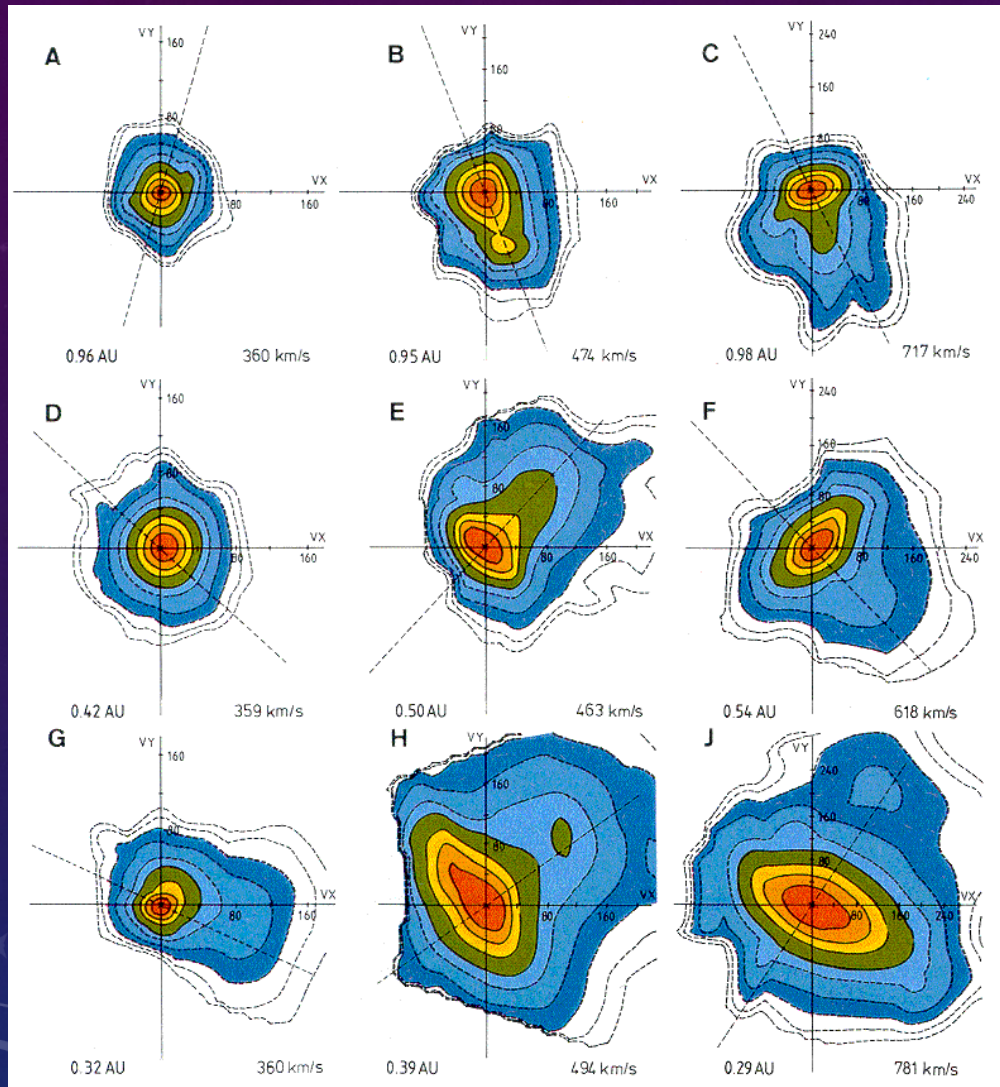
Slow wind:

- $V \sim 600$ à 800 km/s
- $N_e \sim 1$ à 5 cm^{-3}
- $\rho V^2 \sim 2.6 \times 10^{-9}$ Pa
- $T_e \sim 1$ à 2×10^5 K $\rightarrow V_{\text{the}} \sim 2100$ km/s
- $T_p \sim 2$ à 5×10^5 K $\rightarrow V_{\text{thp}} \sim 80$ km/s

Fast wind:

- $V \sim 200$ à 600 km/s
- $N_e \sim 5$ à 20 cm^{-3}
- $\rho V^2 \sim 2.1 \times 10^{-9}$ Pa
- $T_e \sim 1$ à 3×10^5 K $\rightarrow V_{\text{the}} \sim 2500$ km/s
- $T_p \sim 0.5$ à 3×10^5 K $\rightarrow V_{\text{thp}} \sim 40$ km/s

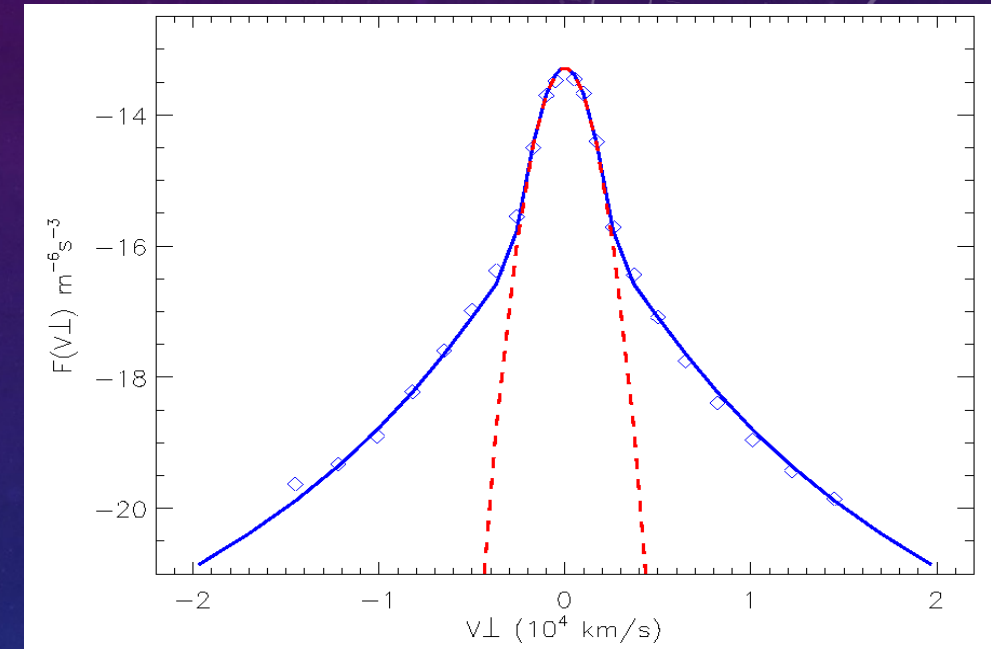
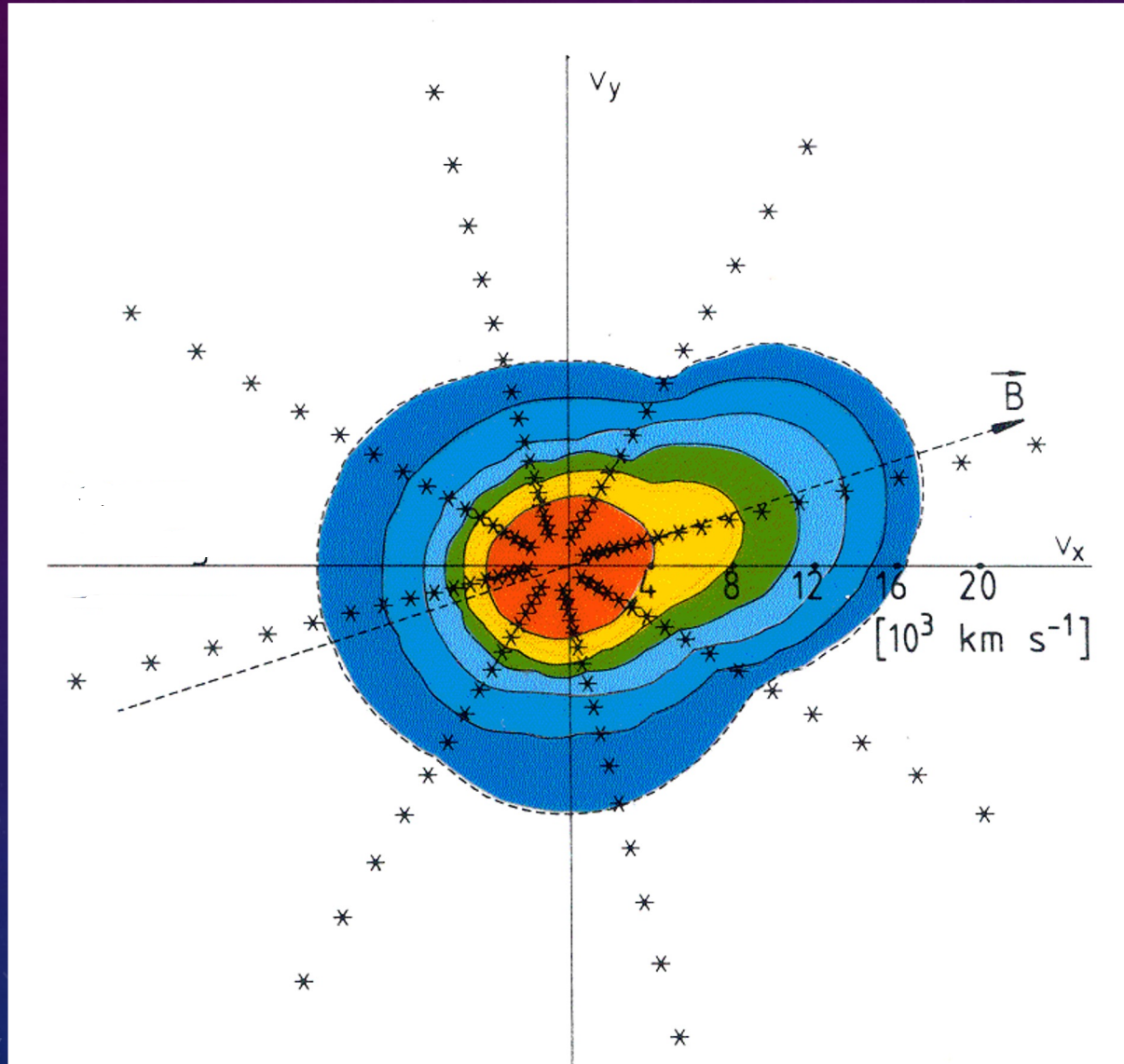
THE SOLAR WIND: MICROPHYSICS, PROTONS



- Temperature anisotropies
- Ion beams
- Plasma instabilities
- Interplanetary heating

Plasma measurements
made at 10 s resolution
(> 0.29 AU from the Sun)

THE SOLAR WIND: MICROPHYSICS, ELECTRONS



- Non-Maxwellian
- Heat flux tail along B

THE SOLAR WIND: MASS LOSS RATE

From the continuity equation:

$$\dot{M} = 4\pi r^2 n m_p u = cste$$

We can evaluate the mass flux by noting that

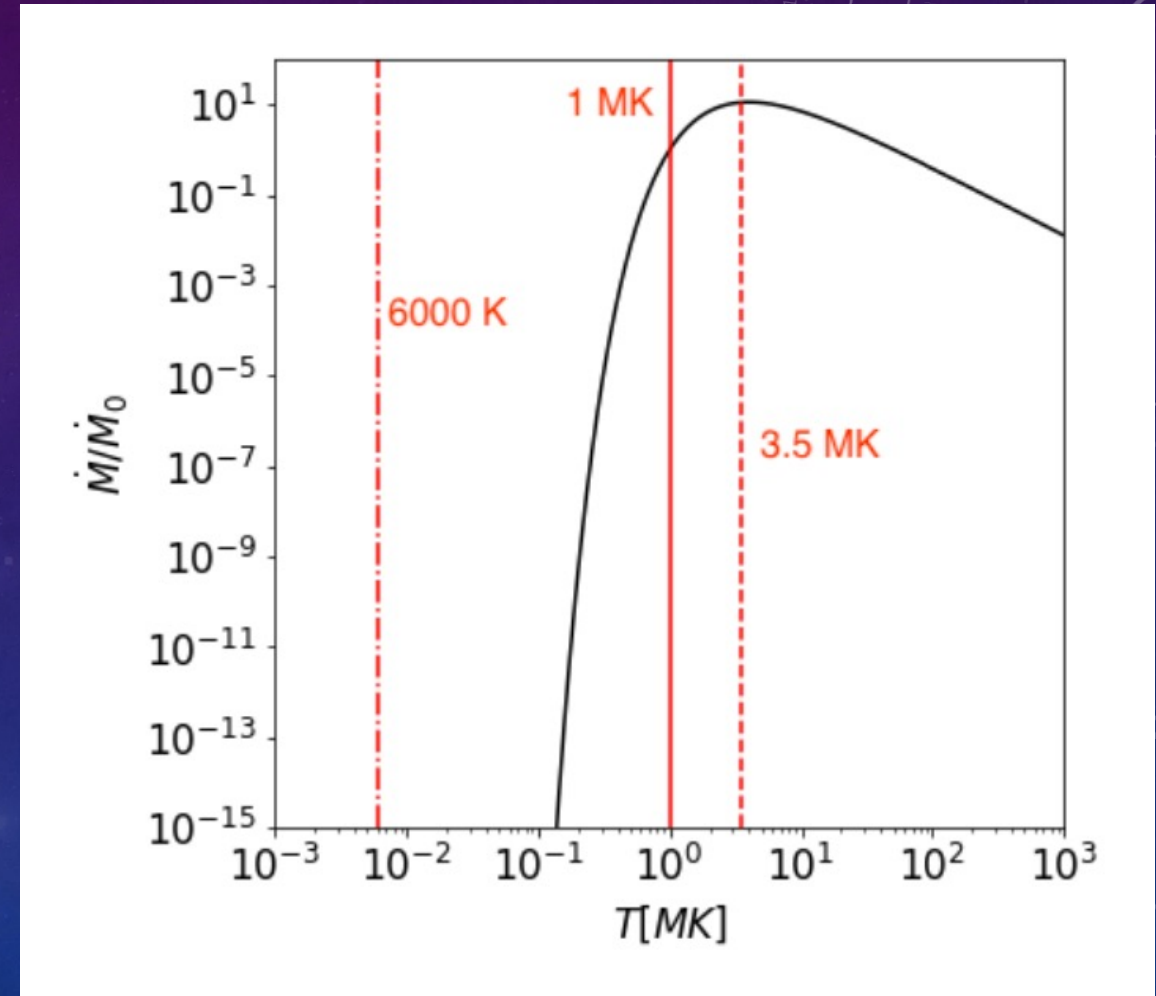
$$u(r \rightarrow 0) \simeq c_s \left(\frac{r_c}{r}\right)^2 \exp\left(-\frac{2r_c}{r} + \frac{3}{2}\right)$$

We obtain

$$\dot{M} \sim 5 \times 10^{10} \left(\frac{T}{10^6 \text{ K}}\right)^{-3/2} \exp\left(-\frac{6 \cdot 10^6 \text{ K}}{T}\right) \text{ kg}\cdot\text{s}^{-1}$$

For $T = 10^6 \text{ K}$ we get 10^8 kg/s (almost exactly what is observed!)

Small fraction of the solar mass per unit of time (equivalent to the mass lost through nuclear reactions)



Extreme sensitivity to coronal temperature

THE SOLAR WIND: POLYTROPIC MODELS

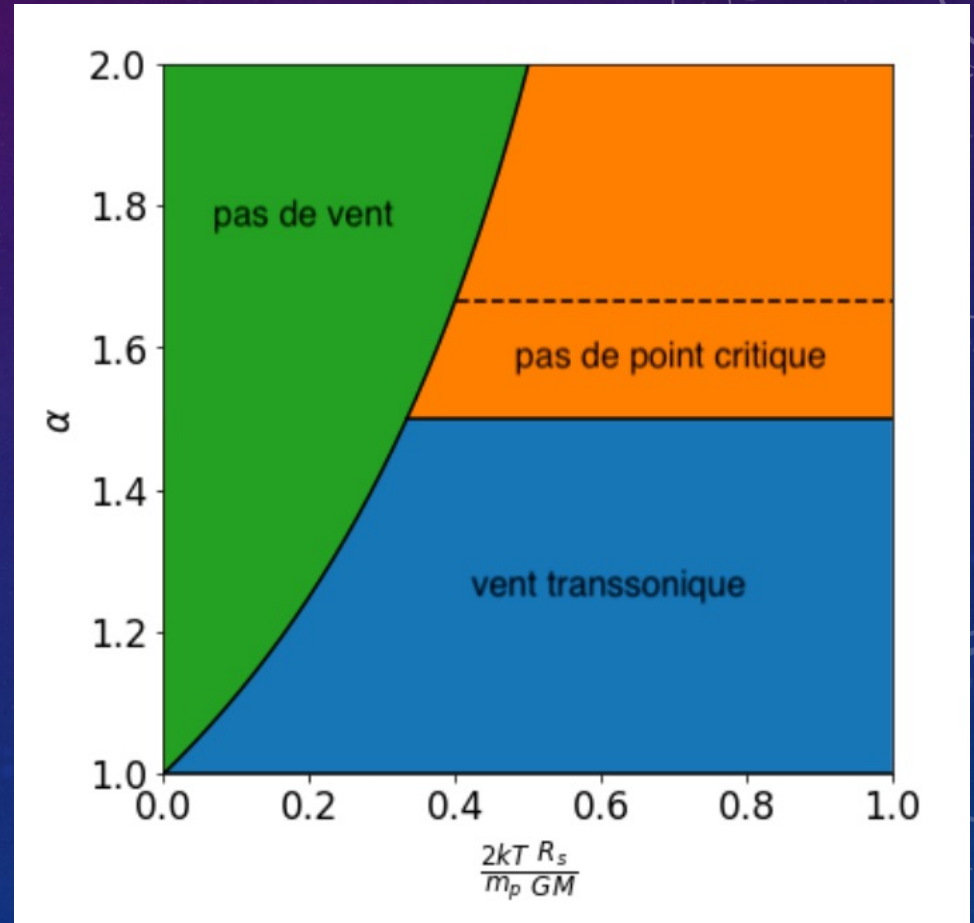
Bernoulli equation

$$\frac{u(r)^2}{2} + \frac{\alpha_e}{\alpha_e - 1} \frac{kT_e(r)}{m_p} + \frac{\alpha_p}{\alpha_p - 1} \frac{kT_p(r)}{m_p} - \frac{GM}{r} = \mathcal{E}$$

Allows one to study the asymptotic behaviour without making a detailed study of the energy balance.

Obviously contains an assumption about the equation describing the heat flux density (closure).

$$\mathcal{E} \simeq \frac{1}{2} m u_\infty^2 \simeq \frac{\alpha_p k T_{p0}}{\alpha_p - 1} + \frac{\alpha_e k T_{e0}}{\alpha_e - 1} - \frac{GMm}{R_s}$$



THE SOLAR WIND: ENERGY FLUX

Energy balance without neglecting convection

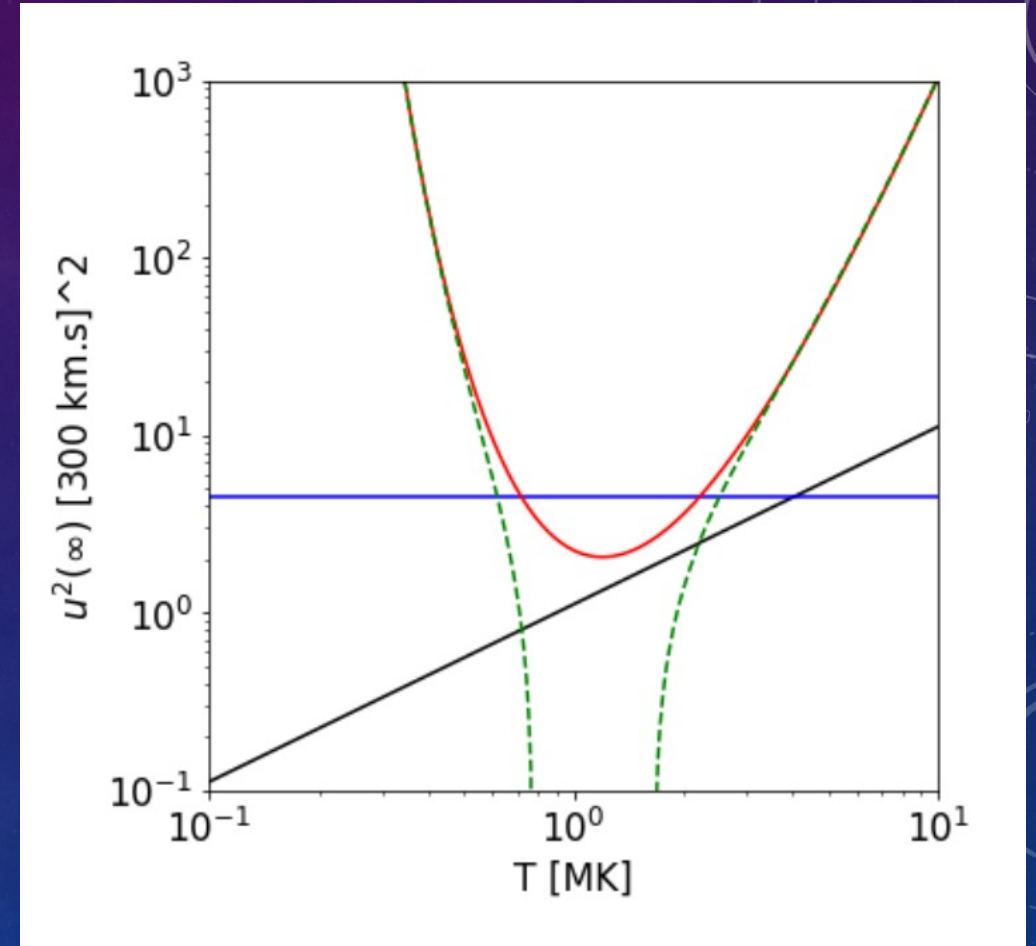
$$\text{div} \left[u \left(nm_p \frac{u^2}{2} + \frac{5}{2} p \right) + j_c \right] = -nu \frac{GMm_p}{r^2} + Q$$

Integrating between two spheres:

$$\dot{M} (\mathcal{E}(r) - \mathcal{E}(r_0)) = \Phi(r) - \Phi(r_0) + P(r, r_0)$$

Neglecting the term $P(r, r_0)$

$$u_\infty^2 = 2\mathcal{H}_0 - u_{lib}^2 - \frac{2}{\dot{M}} \Phi_0$$



There is a lack of energy, $P(r, r_0)$ (such a term is observed in the interplanetary solar wind for protons). Acceleration of the slow wind and the fast wind have different terms (energy requirements, B configuration, etc.).

THE INTERPLANETARY MAGNETIC FIELD: SPIRAL STRUCTURE

Angular speed of rotation of the sun :

$$\omega \simeq 2,9 \times 10^{-6} \text{ rad.s}^{-1}$$

(25 days equatorial period)

In the frame of reference rotating with the sun, the azimuthal component of the velocity field is :

$$u_{\phi} = -\omega(r - a) \sin \theta$$

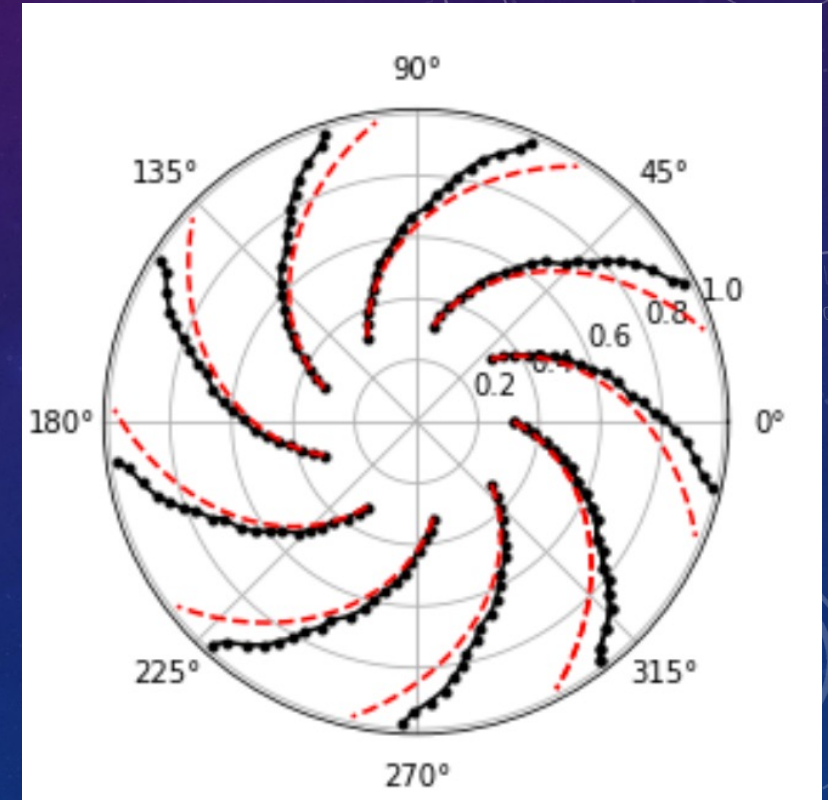
In this frame of reference the B field lines coincide with the velocity field lines (the frost theorem):

The equation for a field line is given by

$$u_0 r d\phi = -\omega(r - a) dr$$

So finally,

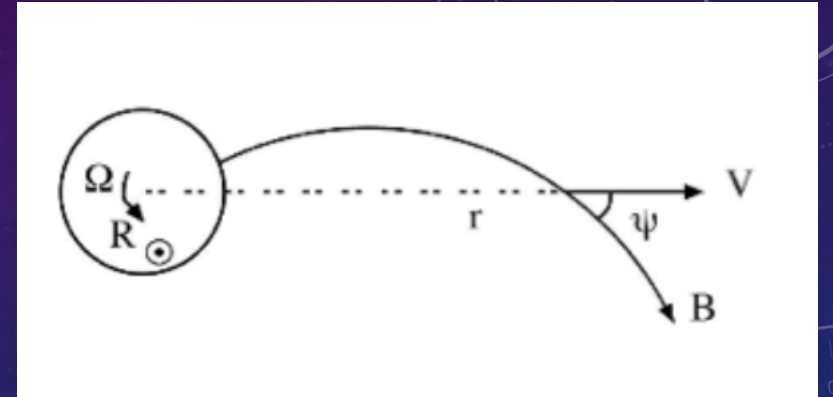
$$r(\phi) - a \ln(r(\phi)/a) = a - \frac{u_0}{\omega} (\phi - \phi_0)$$



THE INTERPLANETARY MAGNETIC FIELD: RADIAL EVOLUTION

The angle between the direction of vector B and the radial therefore changes with the distance from the sun r as follows

$$\tan \psi = \frac{B_\phi}{B_r} = \frac{r \sin \theta d\phi}{dr} = -\frac{\omega}{u_0} (r - a) \sin \theta$$



A constraint on the radial component of B is given by $\text{div B} = 0$

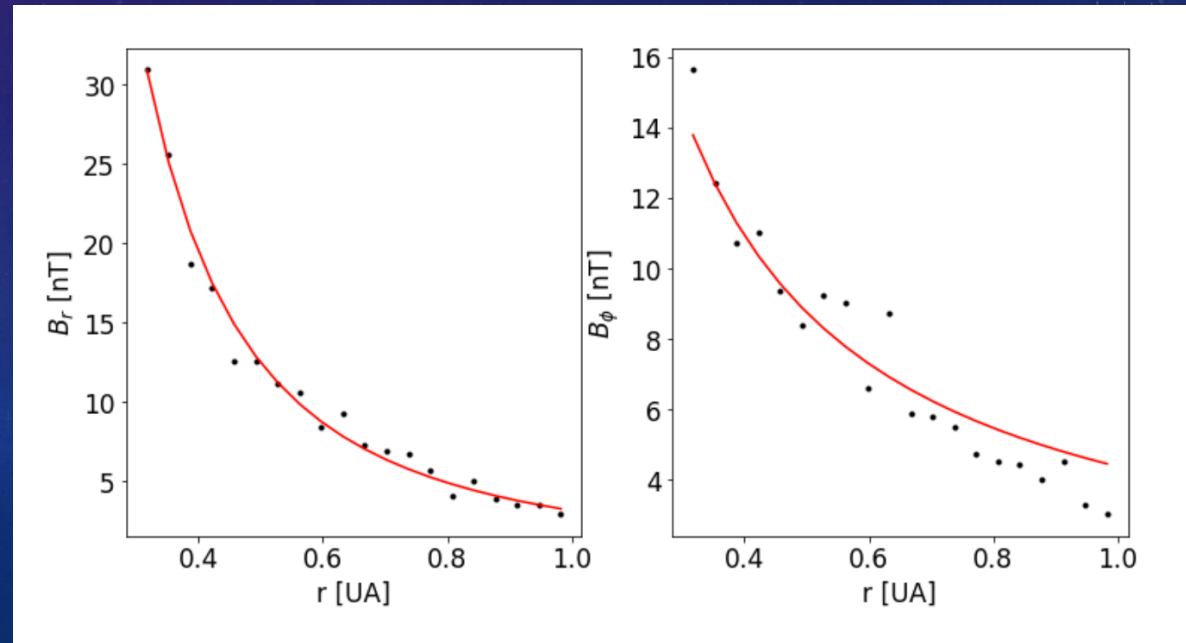
$$B_r(r, \theta, \phi) = B(a, \theta, \phi_0) \left(\frac{a}{r}\right)^2$$

This gives the azimuthal component of B :

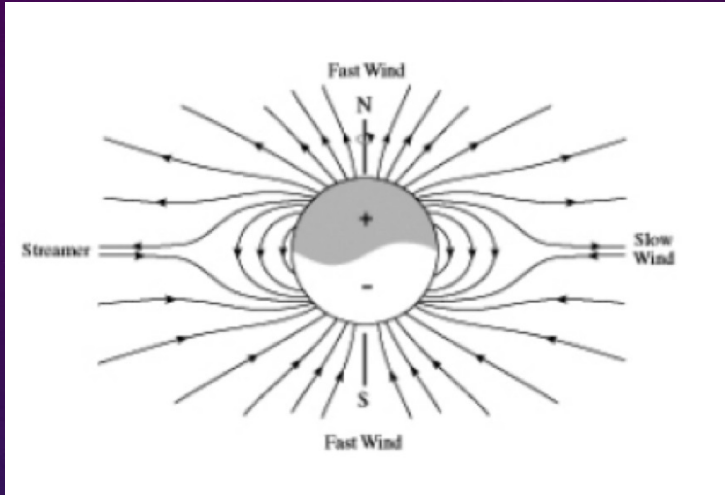
$$B_\phi(r, \theta, \phi) = -B(a, \theta, \phi_0) \frac{\omega}{u_0} (r - a) \sin \theta \left(\frac{a}{r}\right)^2$$

And the modulus:

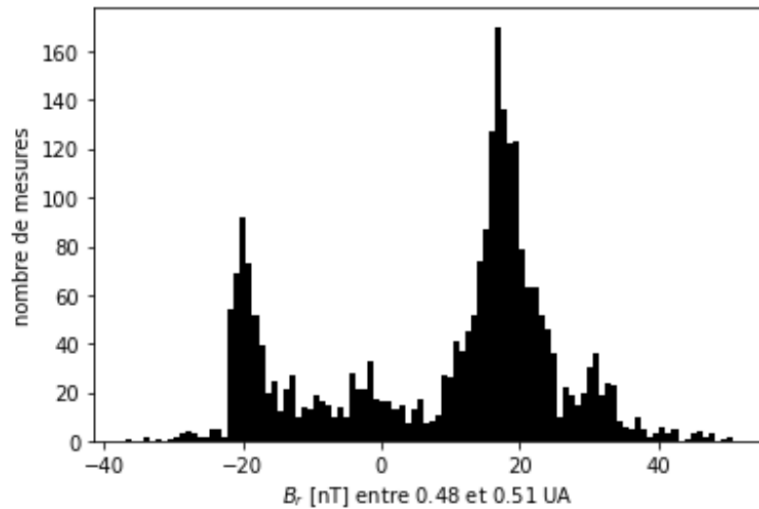
$$|B(r, \theta, \phi)| \simeq B(a, \theta, \phi_0) \left(\frac{a}{r}\right)^2 \sqrt{1 + \frac{\omega^2 \sin^2 \theta}{u_0^2} (r - a)^2}$$



THE INTERPLANETARY MAGNETIC FIELD: STRUCTURE IN LONGITUDE

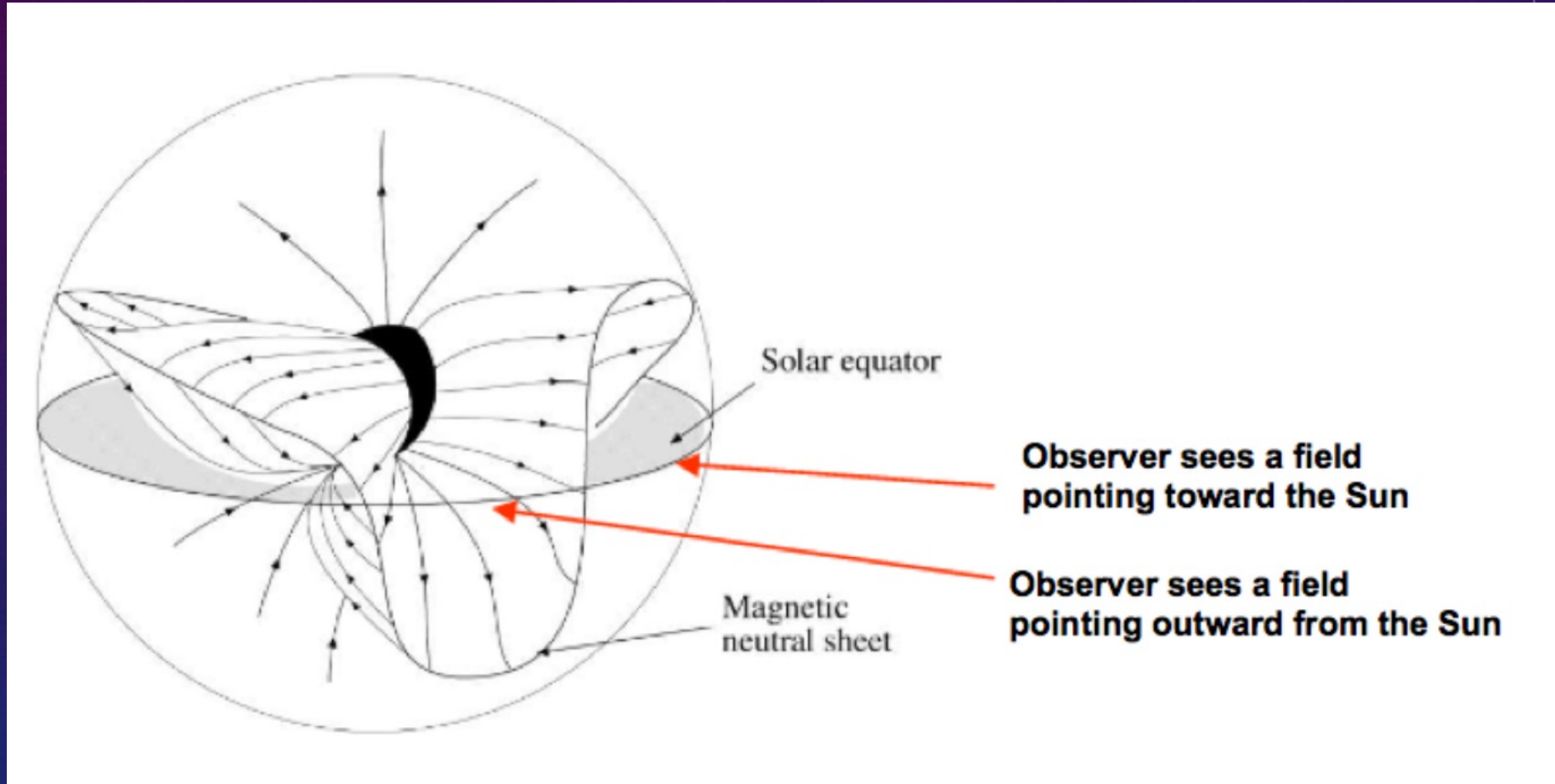


In periods of calm sun (minimum activity): essentially dipolar field + neutral layer (azimuthal current sheet)



Current sheet inclined to the ecliptic plane:
We see alternately a field in the solar direction and a field in the anti-solar direction.

THE INTERPLANETARY MAGNETIC FIELD: STRUCTURE IN LONGITUDE



SLOW WIND, FAST WIND AND MAGNETIC CONFIGURATION

